



HOVERING CRAFT & HYDROFOIL

*Received
Nov. 23, 1964*

THE INTERNATIONAL REVIEW OF AIR CUSHION VEHICLES AND HYDROFOILS



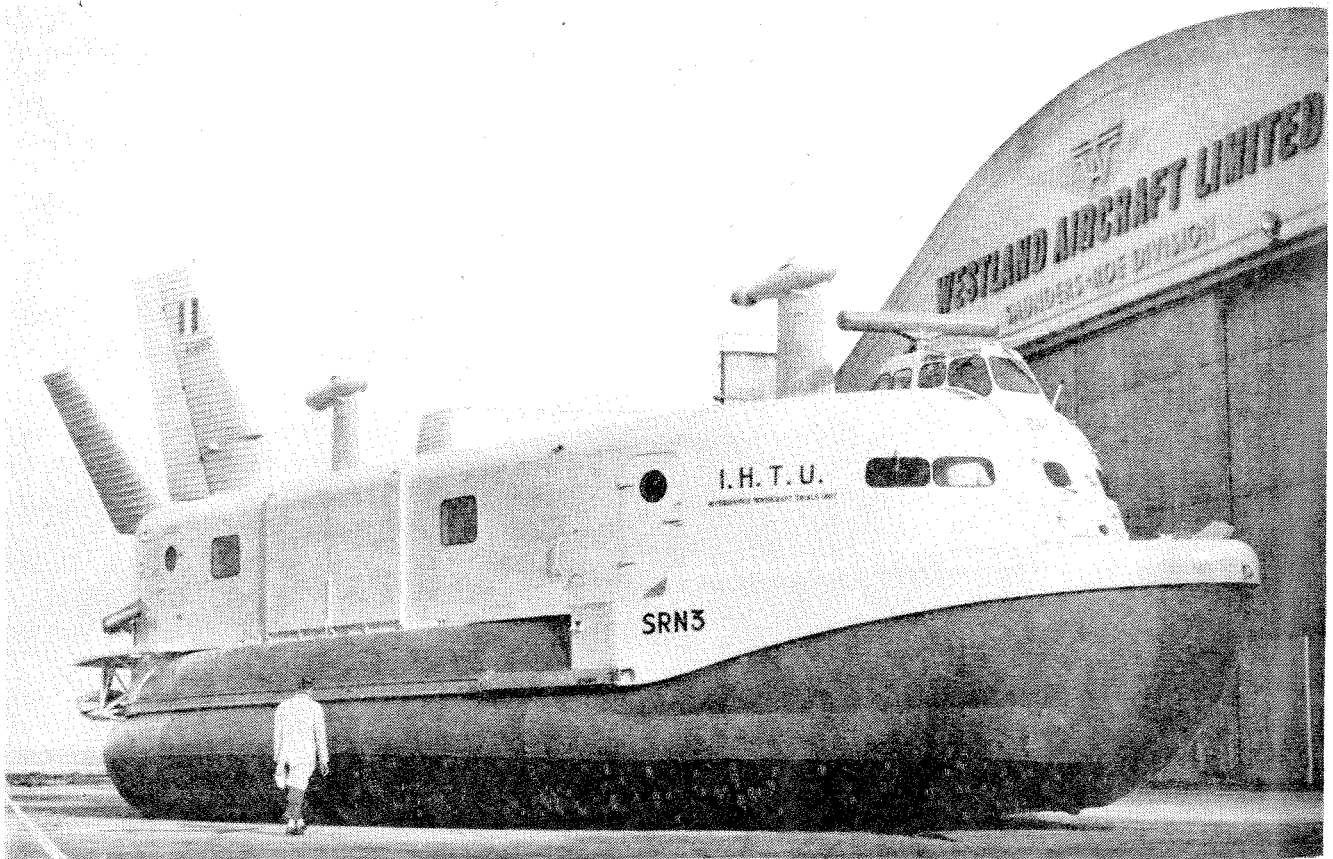
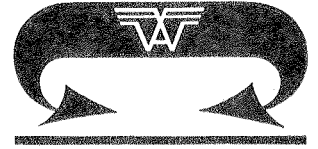
KALERGHI PUBLICATIONS

Volume 3 Number 8
MAY 1964

sustained

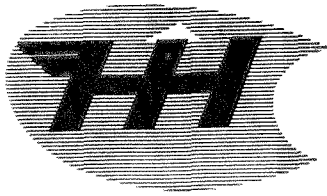
HOVERCRAFT LEADERSHIP

Only four years have passed since Westland's Saunders-Roe Division designed and built Britain's first hovercraft, the experimental SR.N1. Yet to-day, the Company is offering the most advanced range of high-speed, amphibious hovercraft available anywhere. Sizes range from 7 to 37½ tons, and load-carrying capacities from 20 to 150 passengers. In development trials, during which it has to-date covered almost 100,000 passenger miles, the passenger SR.N2 has given the first demonstration by crossing the English Channel, Canada, and operated highly-successful ferry services between Southern England and Northern Ireland across the Bristol Channel. The world's largest hovercraft, SR.N3 (illustrated), has started its proving trials at the British Interservice Hovercraft Trials Centre. A number of over-water and amphibious hovercraft are dependent in future prospects for this type of vehicle, Westland already has the 170-ton, SR.N4 in the advanced project stage. This craft will be used for the fast, all-the-year-round ferry services for passengers and cars across the English Channel.



 **WESTLAND** high riding HOVERCRAFT

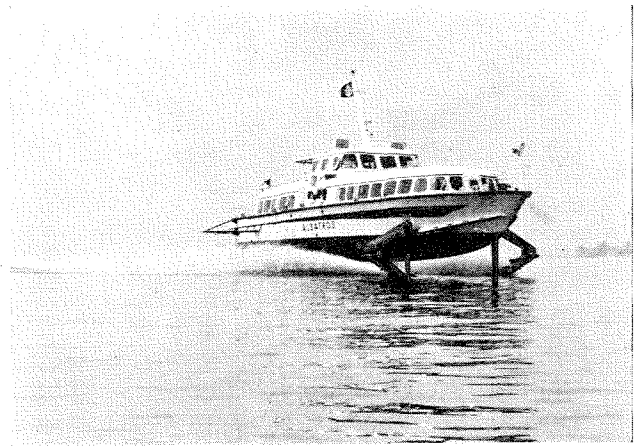
WESTLAND AIRCRAFT LIMITED YEOVIL SOMERSET ENGLAND



HOVERING CRAFT & HYDROFOIL

FOUNDED OCTOBER 1961

First Hovering Craft & Hydrofoil Monthly in the World



The "Albatros", a seventy-eight passenger hydrofoil built by the Leopoldo Rodriguez Shipyard, seen in operation on the Lake of Geneva. For further details of the craft see page 4

PASSENGER REACTION

WHILE most consumer goods can be tested for potential public acceptance before they are marketed—and indeed such pretesting and motivational research has become an exact science—in the transportation field it is only by means of trial and experiment that the public can decide on whether any new method is acceptable or not, for the existence of any form of transport must basically depend upon passenger approval and acceptability. It would be impossible to gauge passenger reaction to travel in hovercraft or hydrofoil by verbal description alone, and it is for this reason that experimental services with such craft can provide invaluable information for potential operators.

At the beginning of May the British public had its first chance of evaluating travel by hydrofoil when the first United Kingdom passenger service was started between the Channel Islands. Hydrofoils are already being used in other parts of the world where all indications point to their ready acceptance by the travelling public, even in areas where fairly rough seas are to be encountered. It is of course too early to assess the reaction in this country but no effort should be spared to make

such an evaluation as soon as possible.

Such information should be made available to all potential hydrofoil operators, for it is only by a spirit of friendly collaboration that the hydrofoil industry can be built up in the United Kingdom. It would be a backward step if needless and unnecessary competition between operators were to hamper this industry in its early days, for although competition is undoubtedly healthy when an industry has found its feet, it can be crippling in the formative days. It might well be a justified criticism that competition in the hovercraft industry started too early at a time when all efforts might have been better directed to putting across to the general public the basic idea of this new form of travel and the benefits it had to offer.

In the method to be adopted of gauging passenger opinion it might be as well to emulate the technique successfully employed by the international airlines who, in the early days of air travel, supplied passengers with questionnaires on their reactions to flying. It might also be an idea to encourage passenger comment on the services they would like to see provided for their comfort within the craft.

IN THIS ISSUE

	People and Projects	4
Discussion on "A Progress Report on Hydrofoil Ships"	Corrosion and Materials Selection Problems on Hydrofoil Craft	5
Britain's First Commercial Hydrofoil Service Operates in the Channel Islands	A Theoretical Approach to the Problem of Harmonic Motions and Forces on a Hydrofoil Boat in Regular Waves	6
	Fifty Four Years Ago	14
		16
		26

COVER PICTURE: *Condor I*, the first hydrofoil to operate a commercial service in the British Isles performing at high speed off the coast of Jersey, in the Channel Islands. Further details of this craft appear on page 14

MAY 1964

VOL 3, No 8

Editor:

JUANITA KALERGHI

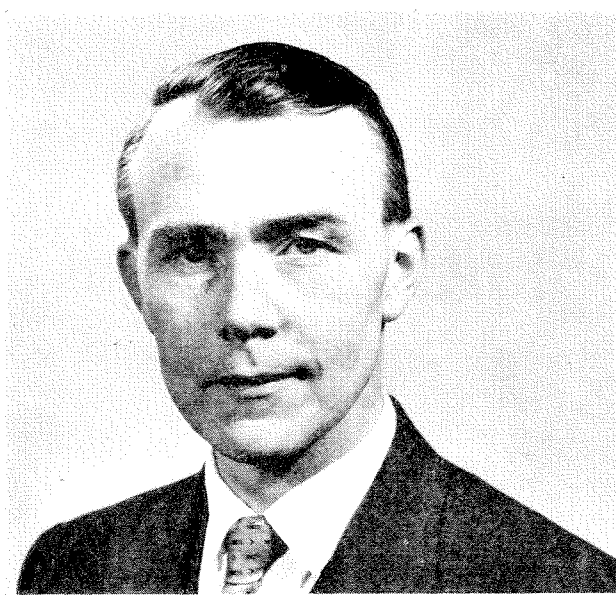
HOVERING CRAFT AND HYDROFOIL is produced by Kalerghi Publications, 53-55 Beak Street, London, W1. Telephone: GERrard 5895. Printed in Great Britain by Villiers Publications, London, NWS. Annual subscription: Five Guineas UK and equivalent overseas. USA and Canada \$15. There are twelve issues annually.

Contents of this issue are the copyright of Kalerghi Publications. Permission to reproduce pictures and text can be granted only under written agreement. Extracts or comments may be made with due acknowledgement to *Hovering Craft and Hydrofoil*.

North American Advertising Representative: W. J. Masterson Co, Box 298, Yonkers, NY. Tel (914) Y05-9793.



E. F. Gilberthorpe, M.I.MECH.E., M.I.PROD.E., M.B.I.M.



R. Stanton Jones, M.A., D.C.A.E., A.F.R.A.E.S.

People and Projects

A daily hydrofoil service has been established between Virgin Gorda (**British Virgin Islands**) and St Thomas (**United States Virgin Islands**) to serve spring and summer guests at the new Little Dix Bay resort.

The craft leaves daily — except Sunday — from St Thomas at 09.00 and 13.13 for Road Town, capital of the British Virgin Islands.

There are connecting services arriving at Virgin Gorda at 12.00 and 16.15. Westbound services are maintained from Virgin Gorda at 08.45 and 13.00 arriving at St Thomas at 11.45 and 16.00. The single fare is \$8.50 (£3).

★ ★ ★

Since 1958 the Italians have been operating a Supramar PT 20 hydrofoil on Lake Garda. Recently the same type of craft, named "**Albatros**" and capable of carrying seventy-eight passengers has been put into service on the Lake of Geneva. The craft was built by the **Rodriquez Shipyard**, Messina, Sicily and was "flown" from there to Marseille encountering waves up to 6 ft en route. From Marseille to Lausanne it was transported by road.

With specially designed foils and its propeller working very near to the water surface the "**Albatros**" can be operated in shallow waters and enter all harbours on the Lake. Trials have proved that the craft behaves as well as the standard PT 20.

The "**Albatros**" is 68.8 ft long, 16.5 ft wide (24.75 ft with its wing-like floats extended), weighs 20 tons, and is powered by a Mercedes-Benz diesel engine. It is expected to carry visitors to the Swiss National Exhibition in Lausanne this summer and will also make short sightseeing trips. Next year it will be used for an express service between Geneva and Montreux via Evian-Lausanne and Vevey.

Two more PT 20 Supramar craft presently under construction at the Rodriquez shipyard destined for Lake Como and Lago Maggiore are to be delivered in Spring 1965.

Mr E. F. Gilberthorpe, MIMech E, MIProd E, MBIM and **Mr R. Stanton Jones**, MA, DCAe, have been appointed Special Directors of Westland Aircraft Ltd. Both will continue to act in their respective capacities of General Manager and Chief Designer at Westland's Saunders-Roe Division where they are concerned with the hovercraft side of activities.

As General Manager, Mr Gilberthorpe was concerned with the production of SR.N3, the world's largest hovercraft, and SR.N5, the first hovercraft to go into full-scale production. Mr Stanton Jones is well known for the part he played in the design of SR.N1, the world's first hovercraft, as well as the SR.N2, SR.N3, SR.N5 and the new 150 ton channel ferry project the SR.N4.

★ ★ ★

Cantieri Navale Rodriquez of Messina have received an order from the Societa Adriatica di Navigazione for a 120 passenger hydrofoil craft for service between the Adriatic port of Termoli and the Termiti Islands. Several daily services will be operated in each direction and the distance will be covered in 40 minutes. The service will commence on June 15th.

★ ★ ★

Ishikawajima Harima Heavy Industries Co Ltd, who have a technical agreement with the General Electric Company of the United States, have recently adapted the CT-58 type turbo-jet engine for marine use, and will mount it in a large hydrofoil craft 20 metres long with a 45 knot maximum speed. The advantage of this engine lies in its light weight. Its maximum output is 1,250 hp or 110 gm/hp compared with 2.3 kg/hp for an equivalent diesel engine.

Discussion on "A Progress Report on Hydrofoil Ships" *

by Norman P. Pascoe, Technical Director, Seaglider Ltd, Farnborough, Hants

INTRODUCTION

I consider Mr Lacey's Report to be of considerable value, particularly at a time when Hydrofoil Craft are receiving renewed and intensified interest from designers and commercial operators on both sides of the Atlantic. Mr Lacey does, in my opinion, adequately and precisely fulfil the objective of his paper and in so doing, makes apparent a number of points worthy of elaboration.

I trust Mr Lacey will forgive me for digressing somewhat from the subject matter of his paper in appending a tabulated summary of principal data relating to a number of noteworthy Hydrofoil Craft in addition to those developed in the USA.

The impetus given to Hydrofoil development in the United States by the US Navy Department compels one to reflect with some envy, and not inconsiderable frustration, upon the relatively poor research and development facilities programme being pursued in this country.

COMMENTS

1. "Fresh"—1 Accident

The relatively minor damage to crew and craft as a result of this accident is a tribute to those responsible for crew safety. I would, however, ask Mr Lacey (a) how it is proposed to retain both stability in yaw and steering effectiveness for a foil system in a broached condition, and (b) why, as a preferred alternative to (a), effort has not been concentrated towards preventing the occurrence of broaching?

2. "Transit" Type of Foil System

It is interesting to note that foils are being developed for "Fresh"-1 which, while providing a desirable flow transition from an all-wetted to a cavitating condition, do nevertheless expose themselves to an intolerable degree of erosion. Does Mr Lacey consider the development of erosion resistant materials (which are likely to yield more acceptable material and dynamic performance) more expedient than the refinement of supercavitating and/or superventilating foil sections already in an advanced state of development?

3. HYDROELASTIC STABILITY

I am encouraged to hear Mr Lacey emphasize the need for a serious study of Hydroelastic phenomena. Although I agree that there is, as yet, no known close correlation between theory and experiment as far as flutter prediction is concerned, I would however suggest that Hydroelastic flutter is more than

just "possible" where high performance wings are concerned. In fact it is evident from experimental data that for rectangular planforms, as the mass ratio is decreased the dynamic pressure at flutter increases and approaches a unity mass ratio asymptotically. A flutter free region is thus indicated for mass ratio less than one. However, theory has shown and experiment has supported, evidence that for as little as 5° sweep, flutter prediction in the normally unswept low mass ratio region results. I am particularly keen to learn from Mr Lacey whether attempts are being made to

- (a) modify planforms;
- (b) improve wing materials;
- (c) effectively change section centre of gravity and elastic axis location by
 - (i) inclusion of high density leading edge inserts,
 - (ii) modification of foil sections,

or a combination of methods (a) (b) and (c) in order to widen flutter free boundaries at high dynamic pressures.

4. COMMERCIAL PROGRESS

I would ask Mr Lacey to indicate the most adverse type of sea conditions likely to be encountered by small commuter craft in the New York City area, and whether such craft are of the "Enterprise" type having submerged foils in Canard configuration. If so, is it considered that fully submerged foil passenger craft show advantage over emerging foil craft for service in this area, and for what reasons? Would Mr Lacey also kindly describe in a little more detail the seventy-five passenger, 35 ton, submerged foil craft referred to in this section of his paper.

5. SUMMARY

The table which follows represents only a small number of contemporary craft of noteworthy design. Limited space prohibits inclusion of many other very interesting craft.

It will be seen that foil systems vary to a considerable extent and it may reasonably be concluded that the systems used are appropriate to the conditions of operation which prevail. I do not think for one moment that designers are still in doubt concerning the choice of an optimum foil configuration for a particular set of operating conditions, and craft. I would appreciate some comment from Mr Lacey in this respect.

I would again like to thank Mr Lacey for his paper which I feel sure must earn him unanimous approval and congratulation.

Craft	Builder	Foil		Speed (knots)	Displ. (tons)	Power (hp)		Control	Application
		Fwd	Aft			Max	Cts		
AG(EH) (USA)	Puget Sound Bridge & Drydock Co	F/S	F/S	50+	320	40,000	28,000	Height sensor (sonic or radar)	Research
HS "Denison" (USA)	Grumman	S/P	F/S	60	80	20,000	14,000	Automatic stability augmentation system	Passenger Ship
"Fresh"-1 (USA)	Boeing	F/S	F/S	up to 100	16	18,000	13,000	Electronic height control	Research
USS "High Point" PC(H)-1 (USA)	Boeing	F/S	F/S	40+	108	—	6,200	Sonic height sensors	Anti-submarine patrol craft
"Aquastroll"	"Aviolanda" for International Aquavion (GB) Ltd	S/P	F/S	32	—	540	—	Not required	Passenger Craft
Hydrofin P20	—	F/S	F/S	45	23	—	1,500	Mechanical Feeler Arm	Passenger Craft
PT 50	Rodriguez Messina	S/P	S/P	40	60	2,700	1,000	Not disclosed	Passenger Craft
"Sputnik" (USSR)	Krasnoye Sormovo, Gorki	S/P	S/P	50	110	3,400	—	Automatic	Passenger Craft
Mitsubishi MH-30 (Japan)	—	S/P	F/S	40	35	—	—	—	Passenger Craft

* "A Progress Report on Hydrofoil Ships" by E. Ralph Lacey was read at the meeting of the Royal Institution of Naval Architects, London, on March 25th, 1964.

Corrosion and Materials Selection Problems on Hydrofoil Craft*

A. E. Hohman and W. L. Kennedy
of
Vought Aeronautics Division
Ling - Temco - Vought, Inc
Dallas, Texas

Introduction

HYDROFOIL CRAFT have been in operation in Europe and behind the Iron Curtain in significant numbers since World War II. Although the United States has built fewer craft, there have been rapid advances in size, speed, and sophistication since 1960. Notable among these is the 80-ton Denison built for the Maritime Administration and the 110-ton PS(H) ocean-going craft to be operational in anti-submarine warfare service in 1963.

As size and speed requirements increase, the requirements for materials to be used in the struts and foils become increasingly more difficult to fulfill. The Bureau of Ships has sponsored a programme* to select materials suitable for use in high performance hydrofoil craft in the 200 to 300 ton class. The ideal material is one exhibiting high strength, light weight, high modulus of elasticity, good ductility, toughness and fatigue life, good fabrication characteristics, corrosion resistance, and low cost. In addition, the material must be available in the sizes required for efficient fabrication.

Within present knowledge, there is no material that can fulfill all of these requirements. Of the available materials, it is not known which ones most nearly fulfill the requirements.

At the beginning of the programme, mechanical and physical property target values were assigned, where possible, based on anticipated structural and fabrication requirements. These are briefly outlined in Table 1. In this discussion of the corrosion properties or properties which are affected by the corrosive marine environment, only materials which measure high in relation to these target values are considered.

Initially, a list of sixty potentially suitable candidate materials was prepared. A literature survey and contacts with data sources reduced this number to the sixteen materials shown in Table 2. The screening tests shown in Table 3 and to be discussed in more detail were performed on these materials.

Fabrication studies of joining methods show welding to be superior to mechanical fastening for typical hydrofoil joints. For this reason, both welded and unwelded specimens have been subjected to the various tests.

TABLE 1 — Desired Material Qualities

Size.....	1.0 in thick x 120 in wide
Strength.....	100,000 psi min. yield (high den. matls) 500,000 psi/lb/in ³ (low den. matls)
Ductility.....	10% elongation in 2.0 in min.
Toughness.....	nil ductility transition temp. 0°F or lower
Fatigue.....	75,000 psi—10 ⁷ cycles unidirectional in sea water (high density matls) 50,000 psi—10 ⁷ cycles unidirectional in sea water (low density matls)
Fabricability.....	above properties retained after processing (welding, forming, machining, etc)

TABLE 2 — Materials Selected for Screening Test Programme Unprotected Plate

Inconel 718	Ti 6Al-4V
K Monel	Ti 8Al-2Cb-1TA
17-4 PH (H1025)	17-4 PH (H1075)
	Berylco 25 Castings
CD4MCU	AM 355
Base Materials for Cladding and Coating	
HY 100	AISI 4330M Epoxy Glass Laminate Claddings
Hastelloy C	Ti A70
	Coatings
Neoprene	Polyurethane

* Revision of paper titled "Some Corrosion Aspects of Hydrofoil Materials Selection", presented at the Nineteenth Annual Conference, National Association of Corrosion Engineers, March 11-15th, 1963, New York, NY

* The work described in this article was sponsored by the Bureau of Ships, Contract NOBs-84593. The opinions and conclusions presented in this article are those of the authors and not necessarily those of the Bureau of Ships or Department of the Navy

TABLE 3—Material Comparison Screening Tests

Mechanical Properties

Tensile Rotating Beam Corrosion Fatigue
Charpy V Notch Unidirectional Corrosion Fatigue
Notched-to-Unnotched Tensile Ratio

Electrochemical Properties

Static Corrosion Unidirectional Corrosion Fatigue
Stress Corrosion Rotating Beam Corrosion Fatigue
Magnetostrictive Cavitation—Corrosion

Jet Erosion Corrosion

Water Wheel Erosion—Corrosion—Cavitation

Fabricability Properties

Machinability
Formability

Weldability
Processability

Test Procedures and Results

Static Corrosion

Military hydrofoil craft may be used on a more irregular schedule than non-military craft. Because of these periods of inactivity, static corrosion data on the materials are important. The trend to retractable foils has lessened the importance of these data somewhat, but the foils may be submerged for prolonged periods to provide additional hull stability.

The materials shown in Table 2 for which static corrosion data were not already available for heat treated, welded, and unwelded conditions were exposed in submerged racks at the International Nickel Company's Harbor Island Laboratory. Two unwelded and two transverse welded specimens were used to simulate the conditions that a foil receiving monthly maintenance would encounter. These specimens were submerged for month long periods below the tidal zone, removed, cleaned, examined, and replaced in the racks. Examinations included determinations of corrosion rate, depth, and extent of pitting and crevice corrosion, galvanic effects of welds, and the amount and types of fouling. Maximum, minimum, and average sea water temperatures for each test period also were recorded.

To establish static corrosion rates in the more conventional manner, duplicate specimens of welded and unwelded materials heat treated to the strength level expected to be used in foil design are being exposed for periods of six months, one, two, and four years.

Average corrosion rates for monthly removal and six-month static corrosion specimens are shown in Figures 1 and 2. The condition of typical specimens and their corrosion rates are presented in Figure 3.

It is important to note that the corrosion rates indicated include material lost through pitting and crevice corrosion. These rates may be misleading if considered as uniform material losses. For example, K Monel appears to be superior to Berylco 25 if rates alone are considered, but examination of Figure 3 shows Berylco 25 to be superior in over-all condition because of the uniform material loss.

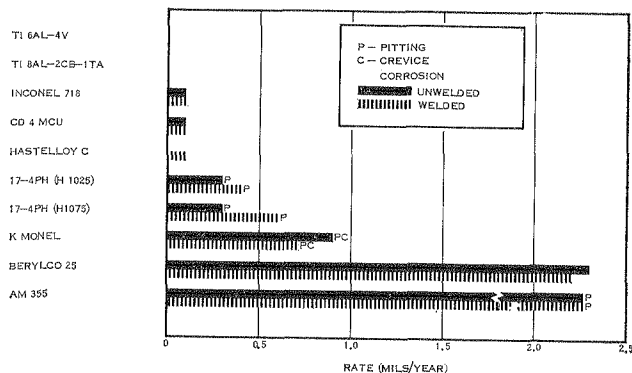


Figure 1. Average corrosion rates for static corrosion specimens removed monthly after sixth removal from sea water at Inco's Harbor Island Laboratory

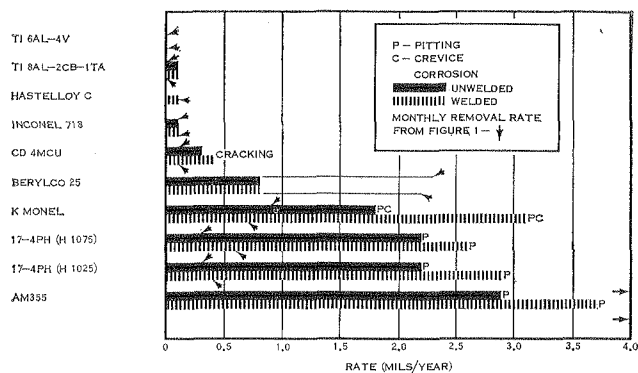


Figure 2. Average corrosion rates for six month continuous exposure of static corrosion specimens in sea water

Corrosion rates for the monthly removal specimens used to simulate a maintained foil are also indicated in Figure 2 which shows rates for specimens exposed continuously for six months. Comparison of the rates indicates that the materials can be divided into three groups as defined by the difference in rates for specimens cleaned at monthly intervals for a total of six times and specimens removed only once at the end of six months. The three groups are (1) both rates no greater than 0.1 mils per year (Ti 6Al-4V, Ti 8Al-2Cb-1Ta, Hastelloy C and Inconel 718), (2) monthly removal rate considerably greater than the six-month rate (Berylco 25, AM 355), and (3) six month rate considerably greater than the monthly removal rate (K Monel, CD 4 MCu, 17-4PH (H 1025) and 17-4PH (H 1075).

From the standpoint of static corrosion, all of the materials in Group One are acceptable for foil construction with or without periodic maintenance. In Group Two, AM 355 is unacceptable because of severe pitting. Removal of the protective oxide film by monthly cleaning of Berylco 25 increased the rate of material loss considerably. The material is attractive, however, because of its anti-fouling nature which would no doubt reduce maintenance requirements. The use of Group Three materials in the heat treated conditions used for this test appears to be unadvisable unless frequent maintenance is performed to remove fouling. Greater confidence can be placed in these trends when data for exposures of a year or more are available and evaluated.

In Figure 4, specimens after six months' continuous exposure are shown before cleaning. The anti-fouling Berylco 25 is clearly visible.

Stress Corrosion Cracking

Stress corrosion cracking in a hydrofoil or strut could easily lead to catastrophic failure. Because it is virtually impossible to construct a foil and strut with assurance that no residual stresses of a magnitude that could cause failure are present, stress corrosion testing became an important part of this programme.

Tests were designed to use stress levels equivalent to 90% of the tensile yield strength. This high stress level was chosen because of the inability to predict accurately what stress level may exist within the foil resulting from welding, machining, or other fabrication procedures. Thus, the ground rule was adopted to eliminate materials which showed cracking at the strength levels necessary to make them attractive from a strength to weight viewpoint. This rule applied to both welded and unwelded material. It was originally intended to test the materials only in the submerged condition, but because of the trend to retractable foils and in further consideration of the parts of the struts which extend above the water line during flight, some materials have been tested in both atmospheric and submerged tests at Harbor Island and Kure Beach.

Five unwelded and five transverse welded 0.050-inch strip specimens stressed to 90% of the 0.2% offset yield strength were exposed with the stressed area immersed in sea water as shown in Figure 5. Three of the five specimens were removed

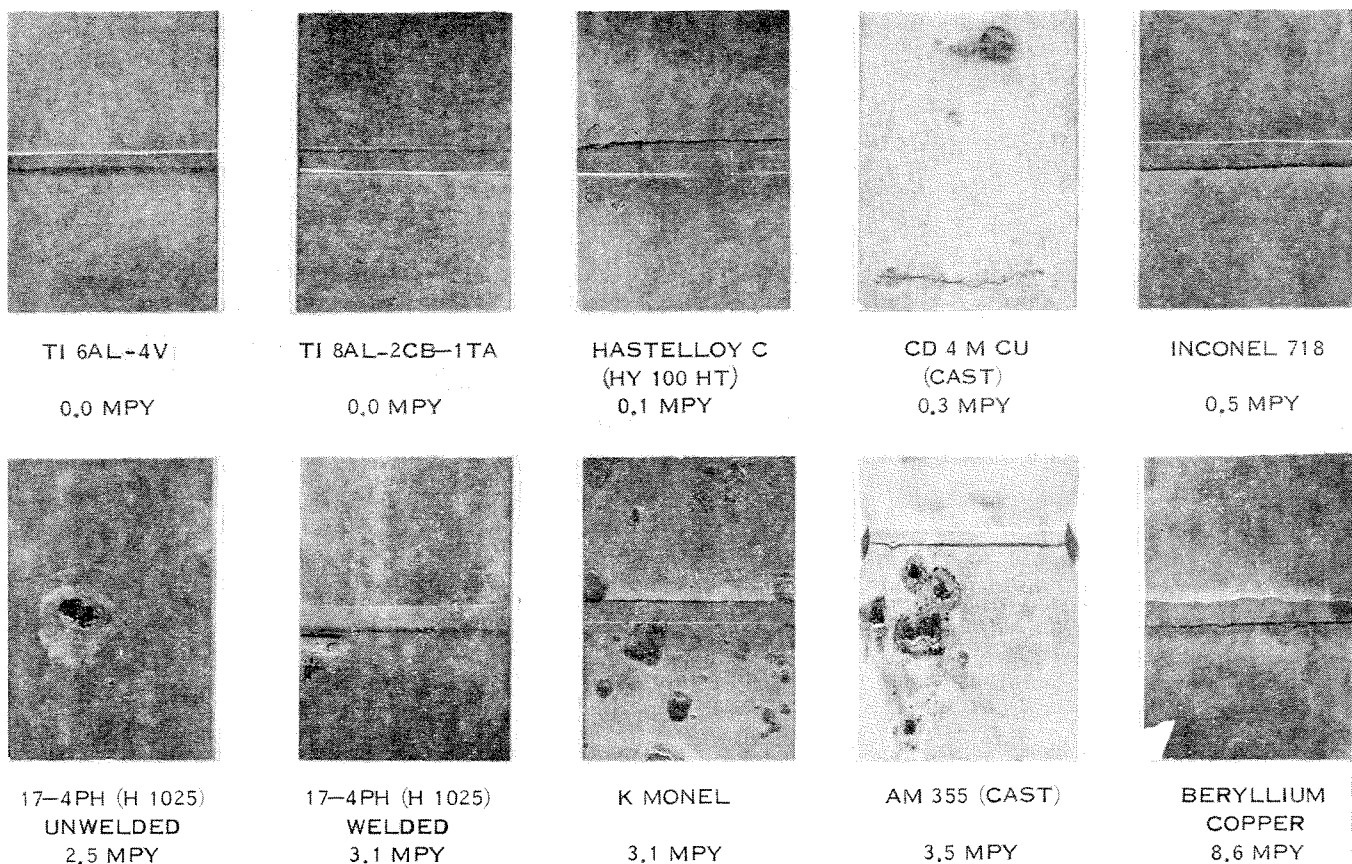


Figure 3. Static corrosion specimens and corrosion rates after six months' continuous immersion in sea water

after six months and placed in the 80-foot lot. This procedure provides data on the effects of wet-dry cycling and any incubation associated with extended submergence. Additional specimens of selected materials have been placed in the 80-foot lot without prior immersions. Test jigs having a fixed length of 7.000 inches were used and specimen lengths determined to place the middle one-third of the specimen under the desired stress.

Circular-patch restrained weld specimens prepared during fabricability studies have also been exposed in the 80-foot lot. Residual stresses in these specimens approach the yield strength of the material in mild steel.¹ The exact stresses are dependent on the shrinkage of the material and the ratio of patch size to plate size. Further evidence that residual stresses can be high is presented in Figure 6. Cracking appeared in one-quarter-inch Ti 8Al-2Cb-1Ta four days after welding and cracked to the extent shown in one month in a laboratory environment. Results of this test should be more representative of material performance in a welded foil than results of the strip specimen exposures.

Stress corrosion failures have thus far been restricted to three materials. Welded AM 355 strip specimens failed from six to sixty-five days after immersion. Four of the specimens had failed after thirty-five days' immersion, all within the highly stressed area. The fifth specimen failed at the water line after sixty-five days. Four unwelded AM 355 specimens (168,000 psi yield strength) failed from eight-five to 157 days. However, all failures occurred at the water line and were attributed to localized corrosion rather than stress corrosion. The fifth specimen has not failed after ten months' exposure.

Four of the welded AISI 4330M strip specimens (160,000 psi yield strength) exposed in the 80-foot lot without previous immersion failed adjacent to the weld after thirty-three, thirty-five, seventy-six and eight-two days. No failures have occurred among the 4330M specimens (185,000 psi yield strength) that were immersed and later placed in the 80-foot lot.

These two groups of specimens were not heat treated and

welded in the same sequence. The immersed specimens were hardened and double tempered after welding. The specimens in the 80-foot lot were hardened and double tempered before welding and then stress relieved. Metallurgical examination of the failures disclosed intergranular failures with branched cracks normally associated with stress corrosion cracking. However, the possibility cannot be overlooked of failure due to cracks developed after welding. Additional testing is planned of welded AISI 4330M specimens exposed to atmospheric, submerged, and controlled environments.

Somewhat conflicting results appear in the case of CD 4 MCu stainless casting alloy. Bent beam stress corrosion specimens 0.050-inch thick showed no failure, while internally stressed specimens intended for static corrosion tests failed by stress corrosion cracking.

The static corrosion test specimens were sand cast in a vertical shape varying in thickness from one-half to one inch and then machined to one-quarter inch thickness. Some of the specimens were distorted slightly indicating internal stress. Heat treatment of the castings included a water quench from 2050 F which has been shown to cause brittle fracture. Cracking of this nature has occurred in short periods in noncorrosive environments.² The failure of several specimens in this programme showed typical branched cracking. Cracking had not occurred after the sixth monthly removal of static corrosion specimens but was present after the seventh. The six-month static specimens also were cracked on removal. The severe quench which in thicker sections causes brittle fracture probably creates a susceptibility to stress corrosion cracking in sections of approximately 0.25 inch and has no harmful effect in sections on the order of 0.050 inches.

Erosion-Corrosion

The effect of velocity on the corrosion rate of materials by water has been the subject of considerable investigation.³ In general, at velocities in the range of 25 feet per second, the corrosion rate of most materials is increased. In addition to

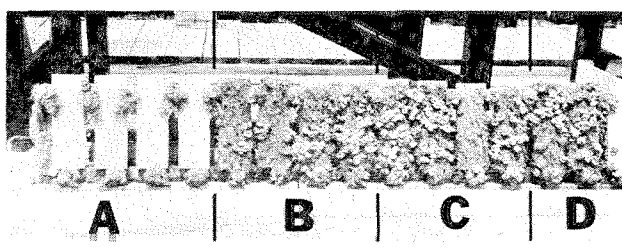


Figure 4. Static corrosion specimens showing fouling after six months' continuous exposure to sea water. Specimens A were beryllium copper; Specimens B were titanium (8Al-2Cb-Ta); Specimens C were titanium (6Al-4V); and Specimens D were Inconel 718

the mechanical action of corrosion product removal, there is an increase in available oxygen. These factors may, in addition to changing the corrosion rate of a material, change the relationship of two materials in a galvanic coupling so that a new galvanic relationship is established. In a similar manner, the galvanic relationship of metals exposed to the high velocity sea water flow and that in a stagnant or crevice area is changed.

A velocity of 150 feet per second corresponding to 90-knot hydrofoil speeds was studied in this programme. The primary objective was to measure metal losses due to the combined effects of high sea water mechanical action and corrosion. In addition, corrosion in crevices adjacent to the area in contact with high velocity sea water had accelerated corrosion rates in some cases. This effect also may become important on foil materials in service. The area being exposed to high velocity water does not necessarily increase in corrosion rate.³ Areas of metal also may become more cathodic to areas of the same metal exposed to a lower velocity with a lower oxygen supply but in which the oxide film is more likely to remain intact.

A test facility for erosion-corrosion testing at Harbor Island was designed and fabricated by Chance Vought. The basic arrangement of the facility and the impingement specimen are shown in Figures 7 and 8. Twelve specimens were exposed simultaneously to the 90-knot sea water for a continuous thirty day period. The 45° impingement angle was selected to minimize cavitation and the water cushioning effect at the point of impact and thus to provide a basis for measuring the effects of erosion-corrosion only.

The metallic specimens were weighed before and after testing, and erosion-corrosion rates calculated. Weekly inspections of surface condition also were made. For metal-coating combinations, the nylon specimen holders were replaced by plates of the material to be coated. These specimens were observed at weekly intervals for erosion damage and loss of coating adhesion.

The average erosion-corrosion rates are presented in Figure 9.

The materials that performed best in both monthly removal and six-month static corrosion tests also exhibited the greatest resistance to erosion-corrosion damage (Ti 8Al-2Cb-1Ta, Ti

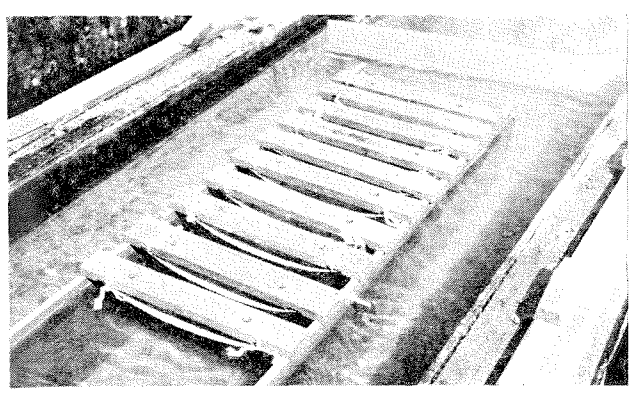


Figure 5. Stress corrosion specimens in submerged test at Harbor Island Laboratory

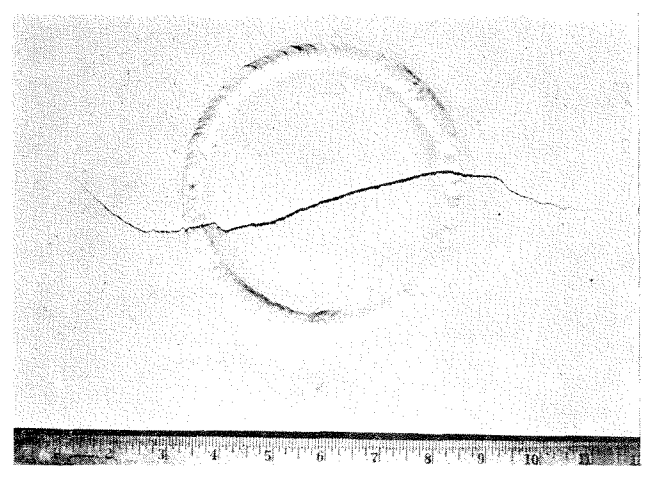


Figure 6. Cracked titanium specimen (8Al-2Cb-1Ta) with a circular patch which was restrain welded. Residual stresses caused cracking in this 1/4 inch titanium four days after welding and cracked as shown here in one month's exposure to laboratory environment

6Al-4V, Hastelloy C and Inconel 718). AM 355 and CD 4 MCu casting materials and commercially pure titanium also suffered little damage during short term tests. Berylco 25 specimens had an eroded surface pattern distinctly different from other materials tested. As expected, both HY 100 and AISI 4330M were severely damaged by the high velocity sea water impingement. This damage appears to be primarily an acceleration of the corrosion rate.

During early phases of testing, crevice corrosion and pitting losses were found to occur to an unusually great extent on the edge and back of Inconel 718, Berylco 25, K Monel and 17-4 PH specimens. An effort was made to determine the extent of this attack and to separate these losses from those on the specimen face due to erosion-corrosion. However, the individual measurement of the two types of attack was difficult due to the specimen configuration. Data obtained were somewhat inconsistent, and thus no quantitative crevice corrosion rate increase can be reported. A few comments concerning the type and extent of damage to each material can be made, however.

Inconel 718 and K Monel were only slightly damaged by crevice corrosion on the specimen edges. The 17-4 PH specimens were severely damaged by crevice corrosion which, in some cases, penetrated through to the back of the specimen. Berylco 25 appeared to suffer approximately equal damage from crevice corrosion and pitting.

A definite statement as to the cause of this damage cannot be made; however, the galvanic effects caused by exposure of separate areas of the specimens to high velocity and stagnant sea water, as mentioned by Copson,³ would seem to be a likely basis for an explanation.

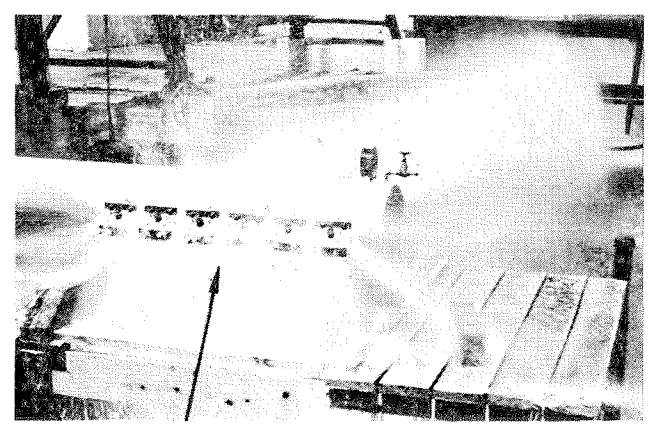


Figure 7. Erosion-corrosion test facility in operation at 90 knots. Arrow indicates specimen holders (see Figure 8)

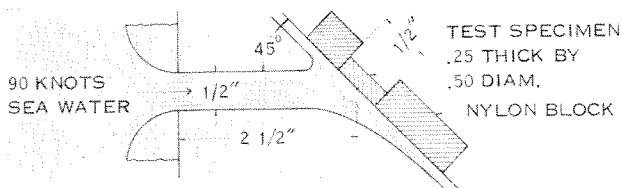


Figure 8. Specimen holders for jet erosion-corrosion testing. Six specimens for each material (three unwelded, three welded) were exposed for 720 hours. Examinations were made for weight losses

These variables were eliminated during later tests by applying a rubber coating over the entire specimen, except the exposed face.

Cavitation-Corrosion

The influence of cavitation on material loss rates from hydrofoils and struts is not yet clearly defined. As in propellers, the existence and severity of cavitation is dependent on design. Thus, with super-cavitating foils, cavitation levels may be present for only short periods during "take off" and return to non-foil borne operation. On the other hand, certain areas of a foil may be subjected to continuous cavitation during flight due to design necessities. In this case, cavitation losses could be of major importance in material selection.

Cavitation itself may remove metal at an alarming rate. It may also function to mechanically remove the oxide films, as in the erosion applications previously discussed, to expose the bare reactive metal surface to the sea water. Metal loss rates are varied by varying the relationship of time of combined cavitation and corrosion to the time in which only the corrosive environment is present.⁴ The rate for a particular material could be varied over a wide range by varying the severity and duration of cavitation in relation to the time allowed for sea water corrosion to proceed. For this reason, this programme has approached the problem by obtaining only a relative cavitation metal loss rate for the materials under two standard conditions in sea water. An estimate of material performance under cavitation probably can be made using this rate and the static corrosion rate for the material.

A few words of caution should be given in respect to cavitation conditions considerably more severe than those used in the magnetostriction test method. In work done at the New York Naval Shipyards Material Laboratory using a rotating disc apparatus to produce cavitation much more severe than that used in this test, titanium was extremely resistant to cavitation and corrosion.⁵ But when an even higher cavitation level was imposed, rapid metal loss occurred. This may be due to a threshold at which the protective titanium oxide layer is removed, followed by more rapid metal removal by a combination of mechanical and corrosive attack.

The relative cavitation-corrosion rates for two standard cavitating conditions were determined during the screening phase of the programme.

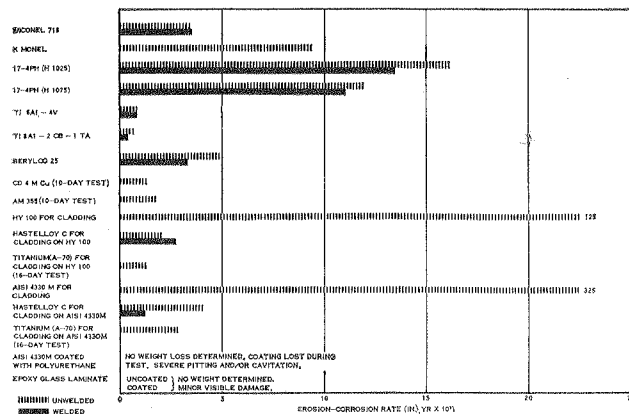


Figure 9. Rates for jet erosion-corrosion in sea water. Exposure was for thirty days at 90 knots

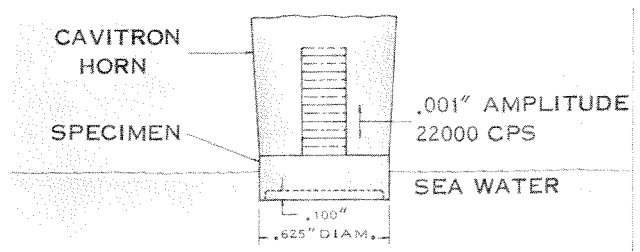


Figure 10. Configuration for cavitation specimen. Each specimen was tested for eight hours, one specimen per material. After test, specimens were checked for weight loss

Magnetostriction cavitation testing was conducted at Chance Vought using Gulf Coast sea water and cylindrical dished type specimens shown in Figure 10. A frequency of 22,000 cps and a double amplitude of 0.001 inches were used. Frequency was monitored by an events-per-unit-time meter and the amplitude checked by microscopic observation. Close control of amplitude and frequency was attained by varying specimen thickness in proportion to material density so that all specimens weighed approximately the same before testing. The sea water temperature was maintained at 72 F (± one degree).

All materials were exposed to a total of eight hours' cavitation. Weights were determined to one-tenth of a milligram after cleaning with distilled water and alcohol and drying in a vacuum dessicator. Weighing was accomplished at 15 minute intervals for the first hour and hourly thereafter.

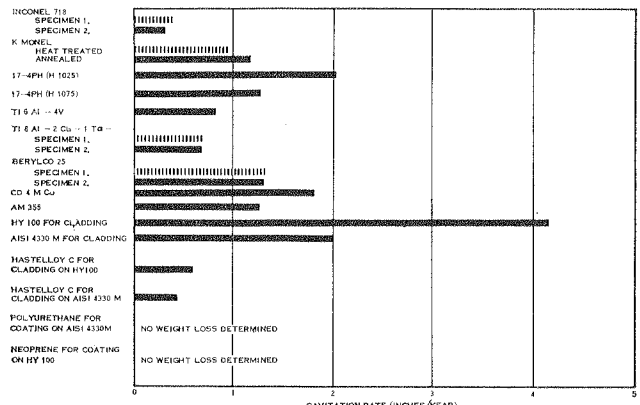


Figure 11. Cavitation rates in sea water. Double amplitude 0.001 inch, frequency, 22,000 cycles per second

Three materials were selected for re-test to check reproducibility of test conditions and data. The results conformed closely to those from the first run.

Magnetostriction cavitation rates are shown in Figure 11. These were determined by plotting cumulative weight losses against exposure time and converting the milligram-per-hour slope to inches per year.

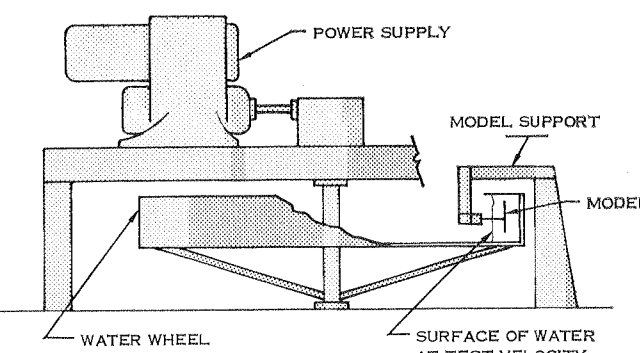


Figure 12. General arrangement of water wheel facility. A five-inch model hydrofoil can be tested at speeds to 100 knots

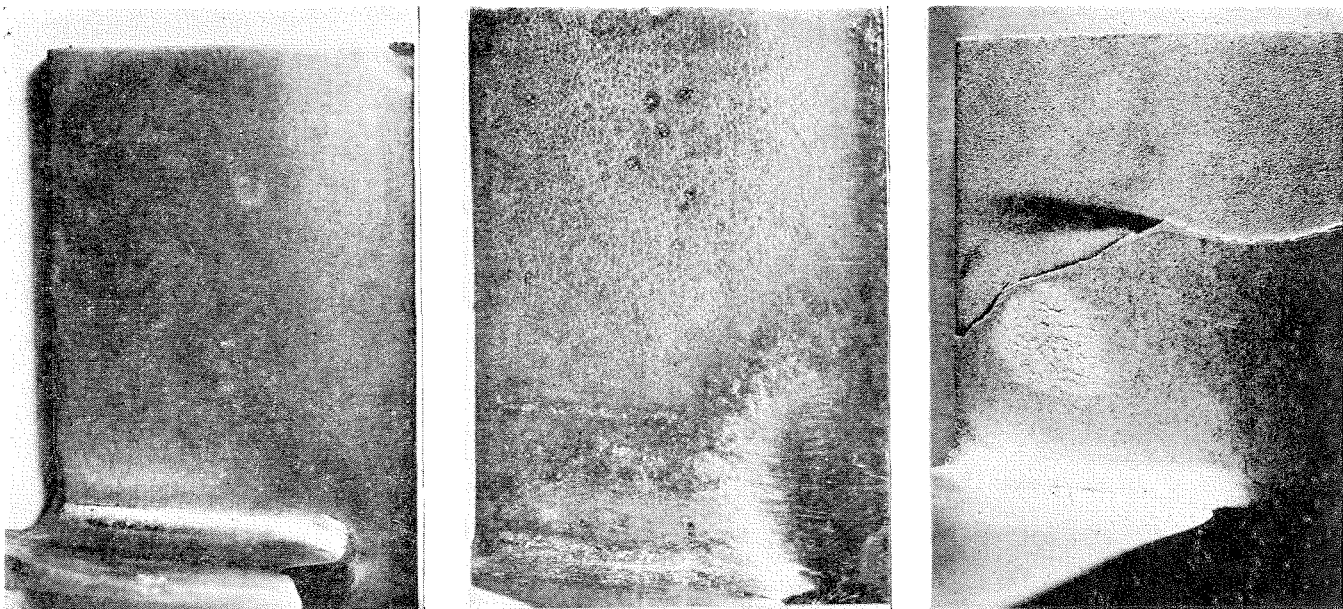


Figure 13. Water wheel specimens after 90 knot tests. Angle of attack was -2° at a 6 in depth. Left specimen is titanium (8Al-2Cb-1Ta) exposed for 100 hours; centre specimen is 17-4PH (H1025) exposed for 100 hours; right specimen is aluminum coated coupon exposed for 50 hours

Materials also were tested for cavitation effects at the New York Naval Shipyard Materials Laboratory using the more severe cavitation conditions. The technique used includes a submerged circular spinning disc 12 inches in diameter and one-eighth inch thick with one-inch diameter specimen inserts. Two specimens are located at each of three radii to produce velocities of 100, 125 and 150 fps. Cavitation is produced by a $\frac{1}{8}$ -inch hole immediately ahead of each insert.

Except for the two titanium alloys, ranking of materials in the rotating disc test was the same as for the magnetostrictive test. The titanium alloys showed only minor cavitation damage at 100 and 125 fps, but specimens exposed to 150 fps showed damage on the order of twenty times that at 125 fps.

Water Wheel

The Chance Vought Corporation water wheel test facility is currently being used to test selected materials by exposure to the local sea water flow environment of a model hydrofoil. This test facility consists of a 12 ft diameter wheel which is arranged for operation in the general configuration shown in Figure 12 and is sufficiently powered to operate at speeds to 300 rpm with a five-inch hydrofoil model. In this manner, local

flow velocities to 100 knots are maintained for long periods with local static pressures varying from atmospheric at the free surface to simulate depths as great as 80 ft. Simultaneous short term corrosive effects are simulated by using sea water.

Three water wheel specimens tested thus far are shown in Figure 13. On the soft aluminum coated specimen, the first to be tested, the area of cavitation damage is clearly visible. Loss of coating from the tip portion of the model was not a result of cavitation. Cavitation damage was not as severe on this specimen in the 40-hour test as damage occurring in only $3\frac{1}{2}$ hours in the rotating disc cavitation test apparatus. The Ti 8Al-2Cb-1Ta specimen is free of damage. No cavitation damage occurred on 17-4PH (H 1025) specimen; however, areas of incipient corrosion are visible near the foil tip and erosion losses are apparent along the leading edge and adjacent to the strut.

Additional testing of these and other materials is planned for a later phase in the programme.

Fatigue

The fatigue problems associated with aircraft structures are well known, especially for wing bending. The problem in

TABLE 4 — Rotating Beam Corrosion Fatigue Test Results — 1450 cpm in Sea Water

Material	Type Specimen	Stress (KSI)	Cycles to Failure $\times 10^{-6}$	Fracture Location	Apparent KT
Ti 8Al-2Cb-1Ta	Unwelded	35	10.1 Avg.*
	Welded	66	0.02	Weld	3.0
Uncoated 433OM	Unwelded	35	0.03
			0.5 Avg.
Coated 433OM	Unwelded	35	6.1†
			10.0*
Coated 433OM	Welded	70	5.0†
			0.23	Weld	1.0
Berylco 25	Unwelded	35	0.02	Weld
			5.5 Avg.
CD 4 M CU	Unwelded	35	1.2 Avg.
AM 355	Unwelded	35	1.0 Avg.
Hastelloy C for cladding on 433OM	Unwelded	35	10.0 Avg.*
			0.23	Weld	2.0
17-4 PH (H 1025)	Welded	73	0.02	Weld
			0.02	Weld
Ti 6Al-4V	Welded	72	0.02	Adj. to Weld	1.5 to 2.0
			2.7	Weld

* No failures. Test to 10^7 cycles maximum

† Failed at edge of coating



Figure 14. Failure of coated specimens (AISI 4330M) after 48-hour exposure at 90 knots. Left: 20-mil Neoprene coating on alkaline cleaned coupon. Centre: 20-mil Neoprene coating on grit blasted coupon with three mils flame sprayed aluminum. Right: 20-mil polyurethane coating on alkaline cleaned coupon

hydrofoil operation is similar but is complicated by the added effect of micro or macro notches formed by corrosion which may result in severe stress concentrations on the structures. In areas of the foil or struts where cycling stresses occur, this corrosion fatigue may be the limiting factor on material usage.

Materials in the last phase of this programme are to be tested in a unidirectional bending test. The target value is 10^7 cycles at a loading of 5,000 to 75,000 psi in tension in sea water. Because of the ready availability at the Harbor Island Laboratory, screening tests have been run using the rotating beam method at a 35,000 psi stress and a load cycling rate of 1450 cycles per minute. This stress level was chosen for the rotating beam test as being approximately equivalent to 60,000 psi unidirectional bending fatigue stress. Results of these tests are shown in Table 4.

To determine the effect of welding on fatigue, duplicate specimens were run stressed at equal percentages of ultimate strength. Based on results shown in Table 4, 17-4PH (H 1025) shows a greater reduction in fatigue strength from welding than does 4330M. Similarly, Ti 8Al-2Cb-1Ta shows a greater reduction in fatigue strength than Ti-6Al-4V.

Coatings

Material and fabrication costs will probably ultimately play an important part in any material selection. Coatings potentially can be applied to base materials with desirable physical properties to impart the necessary resistance to corrosion, as well as erosion and cavitation.

Early exploratory tests showed electroless nickel plate and a flame sprayed ceramic coating to have inadequate adhesion to withstand the standard cavitation conditions created by the magnetrostricture test.

A study of rolled on metal cladding indicated that severe production difficulties would be encountered in rolling on commercially pure titanium. This is due to embrittlement caused by the gettering action of the titanium at the rolling temperature. To alleviate this, elaborate atmospheric control would be required.

Hastelloy C also was considered as a cladding material but was found to have brittle Charpy V notch failures at 0°F after being subjected to the heat treatment of the base material. This is unacceptable because of the possibility of a crack at the surface setting up a stress concentration in the base metal. In addition, a galvanic couple would be created between the cladding and the base metal at the site of a crack.

Elastomeric coatings on base materials such as 4330 steel may be a method to combine strength of the base material with resistance to erosion, cavitation, and corrosion. The elastomeric coatings do not have the disadvantages of the metal cladding in that they can be applied after heat treatment and other processing of the base material is completed. Further, the cost of coatings is considerably less than claddings, and repairs can be made more easily in service.

The elastomeric coatings also have been shown to have potential shortcomings. New York Naval Shipyard tests for resistance to severe cavitation conditions have shown Neoprene and polyurethane elastomers to be undamaged in 72 hours, while hard resinous materials such as epoxy glass laminates and ceramic frit filled polyurethane resins are destroyed within an hour.⁵ However, the 90-knot jet erosion tests on these materials (Figures 14 and 15) show the reverse order of merit. One hundred and fifty hour, 90 knot water wheel tests, which are believed to simulate conditions of jet impact and cavitation expected on typical foils (Figure 16), show that elastomeric coatings perform well even after being broken to simulate damaged areas.

Based on these water wheel tests, the elastomeric coatings may be satisfactory for all conditions encountered on some hydrofoils.

There is no coating presently available to resist both of the more severe conditions presented by the 90 knot, 45° impact angle water jet and the severe cavitation of the shipyard rotating disc apparatus. The improvement that can be offered to the life of a foil by a coating is indicated by corrosion fatigue testing in which life of 4330M steels was increased from 0.5 to 10 million cycles at 35,000 psi stress level.

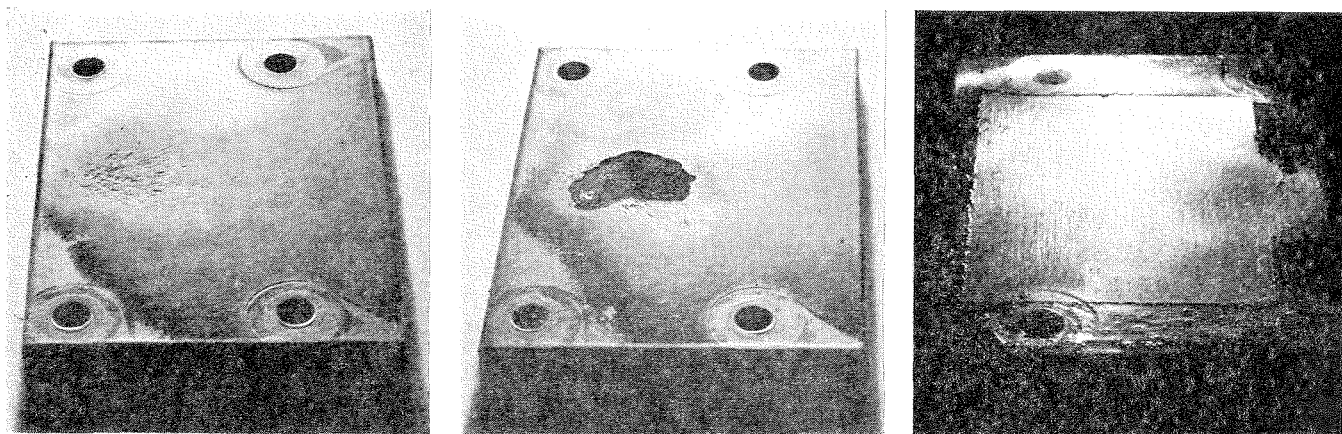


Figure 15. Hard resinous materials such as uncoated epoxy glass laminates (right) and ceramic frit filled polyurethane coating on AISI 4330M (two left specimens) performed well in thirty day, 90 knot erosion-corrosion tests



Figure 16. Polyurethane coated AISI 4330M specimen after 150 hours' exposure in the water wheel (left) and after 50 hours with a break in the coating (centre). Leading edge of the specimen is shown at right

Conclusions

The final evaluation and selection of materials for hydrofoil construction will be accomplished through value engineering by considering all aspects of performance, including the results of the corrosion tests that have been discussed.

In Table 5, the materials have been ranked from the corrosion engineer's view point. Included are brief comments concerning other properties of each material.

No material fulfills all of the requirements for hydrofoil construction. Additional corrosion, fabrication, and mechanical property studies, however, will allow selection of the most desirable materials.

Acknowledgements

The authors acknowledge the contributions of Ivo Fioriti and George Sorkin of the Bureau of Ships whose early recognition of the need for high performance hydrofoil materials helped initiate this programme.

Lee Williams of the Naval Engineering Experiment Station and T. P. May of International Nickel Company's Harbor Island Laboratory were most helpful in securing available data and in establishing test methods. J. Z. Lichtman of the New York Naval Shipyard Materials Laboratory and D. B. Anderson and C. J. Craig of International Nickel Company's Harbor Island Laboratory have contributed helpful suggestions throughout the programme, as well as performing significant test work.

G. A. Starr, chief of Applied Research and Development, H. S. Warkentin, Hydrofoil Materials Research Programme project engineer, and W. H. Sparrow, supervisor of Structures Materials, Chance Vought Corporation, have contributed significant ideas and constructive criticism to the programme since its inception.

DISCUSSIONS

Questions by Robert W. Hinton, 2123½ Ridge Ave, Evanston, Illinois

When rating the alloys for the resistance to cavitation damage after exposure to eight hours of a magnetostrictive test, in inches per year, did you first subtract the incubation period in order to get the rate? If you did not subtract the incubation period, how large was it (the incubation period) compared to the total length of test time for the more resistant materials?

Reply by A. E. Hohman :

The incubation period was subtracted from the rates reported here. After the incubation period, the slope of metal loss versus time of exposure became linear. This linear slope was used as the metal loss rate.

Question by Oystein F. Klingenberg, Langesund, Norway

Has cathodic protection been tried to reduce material loss on foils and propellers on these craft? In Norway, hydrofoil craft operate on fixed routes along the coast, and severe corrosion is reported, especially on propellers. The possible use of cathodic protection of adequate capacity is being discussed at the moment. There seems also to be a need for this type of protection of the hull when the craft is idle, as localised attack on the aluminum hulls is experienced. The use of magnesium or zinc anodes at the mooring site coupled to the ship by flexible lead is suggested.

Reply by A. E. Hohman :

Cathodic protection has not been studied in this programme. Trials by Ionics Corporation have indicated that the current density requirements necessary to protect steel during high speed operation of the hydrofoil would be too high to be practical. During mooring of the craft, cathodic protection would seem to be a practical approach as it is now with conventional craft.

TABLE 5 — Corrosion Ranking of Materials for High Performance Foils

Material	Corrosion Aspects	Other Important Factors
Ti 6Al-4V	High costs, fabrication unknowns, low modulus of elasticity
Ti 8Al-2CB-1TA	High costs, low modulus of elasticity, weld cracking, fabrication unknowns
Inconel 718	Slight crevice corrosion	High cost relative to strength/weight ratio, some fabrication problems
Coated 17-4PH (H 1025)	Crevice corrosion on large bare areas	Questionable coating reliability, heat treatment after welding, low toughness
Coated HY 100	Low strength/weight ratio, coating reliability
Coated 4330M	Stress corrosion cracking	Coating reliability
K Monel	Pitting and crevice corrosion	Low strength/weight
CD4M CU	Stress corrosion cracking, crevice corrosion	Casting material
AM 355	Stress corrosion cracking, crevice corrosion, severe pitting	Casting material

References

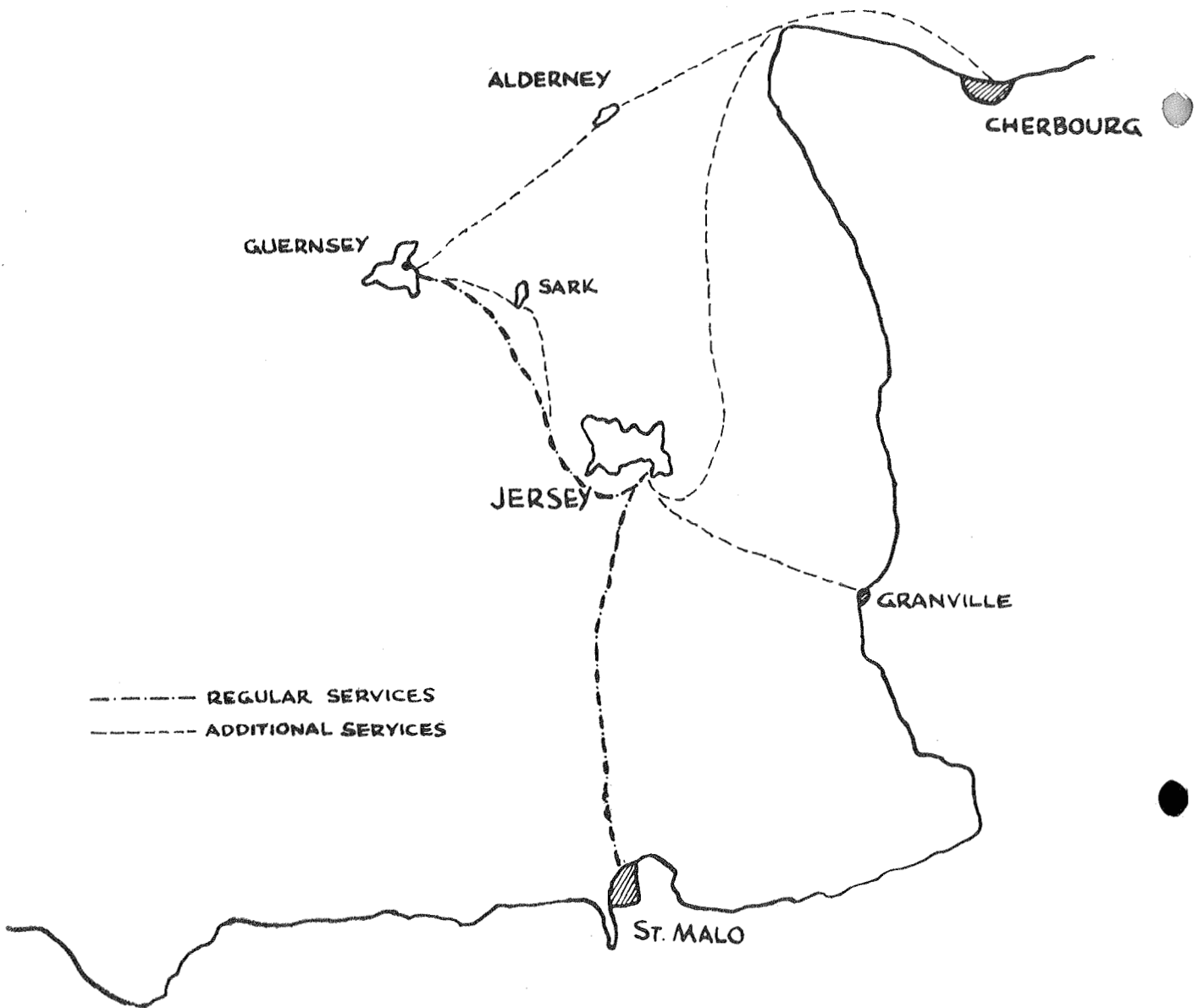
¹ A. V. Levy and H. E. Kennedy. Stress in Circular-Patch Welded Test Specimens, *Welding Journ*, 31 (9), Research Suppl, 402B-405B (1952) September.

² Primate communication, Frank H. Beck, Ohio State University Engineering Experiment Station to A. E. Hohman, December 12, 1962.

³ H. R. Copson, Effects of Velocity on Corrosion by Water. *Ind and Eng Chem*, 44, 1745-1751 (1952) August.

⁴ M. S. Plessett. Pulsing Technique for Studying Cavitation Erosion of Metals. *Corrosion*, 18, 181t (1962) May.

⁵ Lichtman, Kallas, Chatten, and Cochran. Cavitation Erosion of Structural Materials and Coatings. *Corrosion*, 17, 497t (1961) October.



CONDOR I HYDROFOIL SERVICES

INAUGURATED 1st MAY 1964

Britain's First Commercial Hydrofoil Service Operates in the Channel Islands

(From our Special Correspondent)

APRIL 28th marked the occasion of a demonstration, unique in the history of the British Isles. My first glimpse of Condor I, as she lay at anchor, brilliant white in the morning sunshine, was from the air, and I was immediately aware that this was no ordinary ship. On arrival at the jetty where she was moored to a floating pontoon I noted her graceful lines and sound structural design.

After being welcomed aboard by two charming hostesses I settled down in a luxurious seat and could easily have imagined myself aboard a modern jet airliner. Seating and fixtures exemplified the weight saving practices of aircraft design, while the hull structure retained the strong heavy characteristics to which naval architects are so accustomed.

Within minutes of boarding the craft, we were moving

slowly away from St Peter's Port harbour towards open sea. Having chosen a seat immediately above, and within easy view of the main hydrofoil I was ready for action. Twin Mercedes V-12 diesels with gas turbine superchargers purred at steadily increasing frequency as we started our take-off run, and within seconds Condor I was foibleborne, destination St Helier, Jersey.

High winds had encouraged an angry seaway of average wave height 4-5 ft with random waves some 10-12 ft high. These conditions combined with appreciable swell afforded me the unexpected but welcome opportunity of travelling in Condor I under unusually severe sea conditions. It soon became apparent however that sustained high speed (in fact some 30-32 knots) combined with a surprisingly low engine noise level and total absence of vibration was achieved at the expense of a serious reduction in the comfort level one would hope for in a hydrofoil craft of this size. Lateral accelerations were particularly severe and these together with appreciable vertical acceleration reached levels beyond the limits of passenger tolerance. In spite of the fact that we travelled for most of the journey from Guernsey to Jersey in a beam sea, which doubtless contributed largely to the excessive lateral accelerations, the wave encounter rate was sufficiently high (due partly to the high speed of the craft, and partly to unusually short wave lengths) to cause occasional slamming. The occurrence of foil broaching was often preceded by a cyclic shock loading on the main foil. This latter phenomenon although clearly audible did not produce any detectable transmitted shock load on the hull. Under these conditions the craft was contouring the waves to such a degree that any claim to the advantage of hydrofoil travel to those who suffer from sea sickness could not have been justified.

However, I must presume that had fare paying passengers been aboard under these conditions, cruising speed would have been reduced to afford an appropriate passenger comfort level. That this was possible, was adequately demonstrated towards the end of the journey when the Captain reduced speed on his approach run into St Helier.

In spite of these adverse sea conditions the craft completed the journey from Guernsey to Jersey within her scheduled time at an average speed of about 30 knots, a performance which is indeed a tribute to her designer, builder and crew alike.

Before going on to describe some very interesting technical details of this craft, I would summarise my impressions of the demonstration run by saying that at *high speed in severe seas*, Condor I

(a) performs safely, but at the expense of passenger comfort.

(b) demands excessive crew concentration which inevitably gives rise to crew fatigue, but at *appropriately reduced speed*, performs well on all accounts.

It is interesting to consider whether there is a significant difference in expected foil life between constant use at 32 knots and constant use at say 20 knots, and whether there is any sound economic reason for operating the craft at slightly reduced speed.

At a press conference held after the demonstration it was indicated that Condor I can operate at a passenger fare below that of air travel over the same route, and can offer comparable journey duration and comfort. I was a little disappointed that no mention was made of Baron H. von Schertel, to whom much credit and admiration is due for the design of this craft.

Some Background Details

Condor I is a type PT 50 hydrofoil craft, constructed at the Cantieri Navale Leopoldo Rodriguez, Messina, for Condor Ltd of St Peter's Port, Guernsey. Leopoldo Rodriguez, who is Managing Director of the shipyard, has earned himself the reputation of being the world's leading authority in the construction of commercial hydrofoil passenger craft, of which Condor I is typical. Some fifty to sixty vessels of this type have been built at Messina over the past six years.

Mr Peter L. Dorey, the Managing Director of Condor Ltd is a man of considerable energy and insight, and together with the Commodore Shipping Co which owns a principal share

holding in Condor Ltd, feels that we may look forward to a very bright and interesting future for hydrofoil passenger service in the Channel Islands. Condor Ltd will be considering extending their hydrofoil service to include Granville, Cherbourg as well as the Islands of Sark and Alderney depending upon tide conditions and traffic demands. The present service includes Guernsey, Jersey and St Malo.

I think it would be reasonable to assume that the readers of this journal are thoroughly conversant with the principles of hydrofoil flight. I would, nevertheless, take this opportunity to deplore the references which are all too frequently made in the national press to boats which travel on "skis". The conventional planing craft has of course been subject to this phenomenon for a considerable number of years, and it is to be hoped that any hydrofoil craft (with the possible exception of the Grunberg type) will be designed so that its foils are NOT under any conditions able to act as "skis".

It is perhaps most convenient to briefly summarize the technical specification of Condor I as follows:

Dimensions :

Length overall	91 ft 6 in
Beam	20 ft
Width across foils	35 ft 2 in
Draught at anchor	11 ft 10 in
Draught cruising	4 ft 11 in

Performance :

Take off speed	16 knots approx
Cruising speed foibleborne	33 knots
Maximum speed	38 knots
Fuel consumption	75 gals per hour (16.3 lb per nautical mile)

Displacement : (Fully loaded) 60 tons

Payload : 25,353 lb

Power Unit : Two Mercedes Benz 4 stroke, single acting V-12 diesels delivering 1,350 hp each at 1,500 rpm. Supercharged by Brown Boveri gas turbines rotating at 34,000 rpm.

Seating :

Passengers	110-130
Crew	6

Range : 377 nautical miles

Proposed Schedules :

Below are typical schedules proposed for the commencement of service on May 1st, 1964.

Guernsey dep 7.00 am	Jersey arr 8.00 am
Jersey dep 8.30 am	St Malo arr 10.00 am
St Malo dep 10.30 am	Jersey arr 12 noon
Jersey dep 4.00 pm	St Malo arr 5.30 pm
St Malo dep 6.00 pm	Jersey arr 7.30 pm
Jersey dep 8.00 pm	Guernsey arr 9.00 pm

A new type of Decca transistor marine radar which has been installed in over 1,500 vessels since it was introduced a year ago is in use in the craft. The D202 is a light weight, low power consumption equipment with a 4 ft slotted waveguide aerial weighing 77 lbs. The display provides an effective $7\frac{1}{2}$ in diameter viewing area and incorporates six range scales from $\frac{1}{2}$ to 24 nautical miles; two pulse lengths are automatically switched with range scale—a 0.1 microsecond short pulse for high picture quality in confined waters and a 0.5 microsecond long pulse for solid echoes at long ranges.

Electrical equipment in the craft includes a Marconi Marine Fulmar transmitter, and a Guardian receiver providing short range intermediate frequency radiotelephony communication.

It only remains for me to say that I was very favourably impressed by the demonstration of Condor I and that I sincerely hope Condor Ltd will, in the near future, extend both the size of their hydrofoil fleet, and the extent of their services. In this respect I wish them every success.

A Theoretical Approach to the Problem of Harmonic Motions and Forces on a Hydrofin Boat in Regular Waves

Christian Pringiers
Naval Architect

AMRINA - AMSNAME - AMNECI

1. Introduction (ref. [1] and [2])

MR. Hook's system having been thoroughly explained in these pages by the designer himself and Mr. Vintonon, it will be sufficient to consider the schematic sketch, fig. 1, to be reminded of the general principles of mechanical feelers. The same drawing gives also most of the symbols which are used in the following calculations.

As already known, the main characteristic of Mr. Hook's invention is that his height sensor gives non-linear inputs to the forward, incidence controlled, foils, the light spring-heel device acting as a H.F. impulse-filter.

It is therefore obvious that a complete mathematical solution to the problems of motions of "Hydrofin" boats would require rather sophisticated methods of calculation, making the use of analog computers practically unavoidable.

This paper is more limited in scope. We shall limit ourselves to some typical cases, leading to most representative orders of magnitudes, and based on reasonable approximations which are, in any event, always helpful in speeding-up the first steps of the project.

2. The periodic forces in sinusoidal waves.

2.1. Some general considerations

It is well known that hydrofoil craft supported by fully submerged foils do not obtain sufficient stability from the variation of lift as a function of the immersion. Incidence-control is a necessity from which, forces arise which are a function of the angle of attack. All other forces developed by heave, pitch and orbital motion in the waves are also a function of this angle, so that we note that the problems of fully (and rather deeply) submerged foils are basically simpler than those of surface piercing foils, for which every motion of boat and surface introduces two terms.

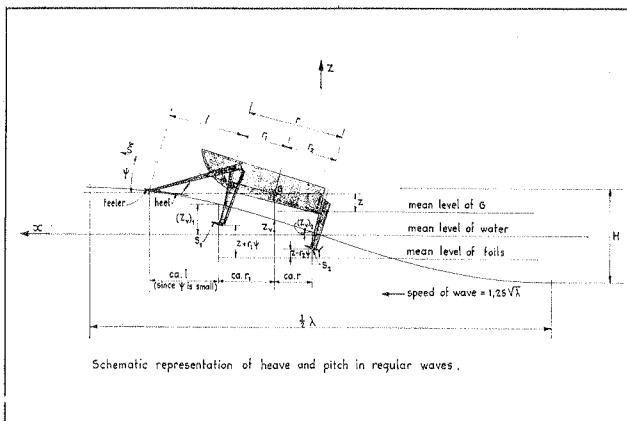


Figure 1

When incidence variations are not too rapid, the lift increment is given by:

$$C'_L \frac{1}{2} \rho V^2 S \cdot \Delta \alpha$$

where C'_L is the lift slope and α the mean angle of attack (for other symbols, see the list at the end of the paper).

There are different lift slope formulae, three of which are given in ref. [3]. One of them is reproduced here to illustrate the influence of the different parameters:

$$C'_L = \frac{2 \pi A}{A + 2} \left(\frac{a_2}{a_1} \right) 1,1 \cos \Lambda$$

where A = aspect ratio

Λ = angle of sweep-back

$\frac{a_2}{a_1}$ = a corrective factor, increasing with A and with the ratio submergence on chord.

We note that the lift slope increases with the aspect ratio and the immersion, but decreases with the angle of sweep.

It must be noted that such an expression is valid only in the case of so-called "quasi steady" lifts, i.e., for rather slow oscillations. Owing to the time-lag in the activation of the increment or decrement of circulation, the complete formulation of the lift slope implies a corrective factor of the form:

$$\frac{M}{M + jN}$$

which corresponds to an attenuation factor of modulus $\sqrt{M^2 + N^2}$ combined with a phase lag, the tg. of which is given by $\frac{N}{M}$.

The parameter governing this phenomenon is generally called k , and is expressed by:

$$k = \frac{\omega s}{V} \quad \text{or} \quad k' = \frac{\omega s}{2V}$$

where s = chord length.

Table 1 - Characteristics of a small Hydrofin-boat (K2)

Length over-all	6,10 m.
Weight empty	1100 kg.
All-up weight	2000 kg.
Power	65 - 95 hp.
Passengers	6
Speed	26 - 32 kn.
Distance between foils and keel	abt. 1,00 m.
Min. depth of submergence in platforming	abt. 0,40 m.
r_1	2,10 m.
r_2	2,70 m.
l	2,60 m.
S_1	0,30 m ²
S_2	0,16 m ²
i	1,50 m.
i_a	0,30 m.

Table 1

A high ω and large $\frac{s}{V}$ ratio meaning a small lift variation and a large lag, the question is, of course, to determine for those variables the practical order of magnitudes which are likely to occur in the following calculations.

Table 1 gives the main particulars of one of the small "Hydro-fin" boats. It can be seen that waves of about 0,60 m. (2 ft.) may be absorbed in level platforming (1). We shall therefore start our investigation on the basis of higher waves likely to be encountered by the craft, which will, ideally, contour them with the minimum pitch and heave necessary to avoid slamming. Let us assume a wave height of 1,00 m. and a wave length of 36 m., a combination which is, statistically, quite acceptable. The boat, flying at 30 knots against such a sea, will meet the waves at a circular frequency of encounter $\omega = 4$, corresponding to the rather high figure of 0,64 cps. The mean chord length being 0,20 m. and the speed 15,45 m/sec., we find $k = 0,052$.

Plenty of highly specialized studies have been published, most of which give pure theoretical evaluation of the $(M + jN)$ factor, for typical cases such as sinusoidal gusts, trochoidal waves, heave and pitch, for both sub- and supercavitating foils. Depending on the basic assumptions and simplifications, the results vary rather largely, and it remains outside the scope of this paper to discuss the different theories. However, a general conclusion may be drawn from all of them for the example outlined above (2): the attenuation as well as the phase-lag are certainly negligible, i.e., respectively less than 3 per cent and 5 degrees, these values, especially the second, being as pessimistic as possible.

Now for bigger craft of the same speed, the chord length will be larger, but the frequency of encounter for contoured waves will decrease approximately in the same proportion, so that it will not be necessary to introduce special corrections in scaling-up.

2.2 The different possibilities of variation of the angle of attack.

2.2.1. Incidence control

Fig. 2 gives the details of the linkage between feelers and foils. The relation between the relative vertical displacement feeler — foil ($Z_p - Z_l$) and the corresponding incidence variation may be written:

$$\Delta \alpha = \frac{Z_p - Z_l}{K}$$

where: $K = 1 \times \frac{m}{u} \times \frac{q}{n}$

2.2.2 Orbital motion and heave

The circular motion of the water particles may be split up into a vertical and a horizontal oscillatory translation. Both of those movements are approximated by sinusoidal functions of amplitude $\frac{H}{2}$ for the surface: $Z_v = \frac{H}{2} \sin \omega t$ (as seen by an observer on board the boat).

At a given instant, the relative speed wave-foil is defined by:

a vertical component: $\dot{Z}_v - \dot{Z} = \mu \frac{\sigma H}{2} \cos \omega t - \dot{Z}$
 a horizontal component: $\Delta V = -\mu \frac{\sigma H}{2} \cos \chi \sin \omega t$

where \dot{Z}_v = vertical speed of the water
 \dot{Z} = vertical speed of the foil
 σ = own circular frequency of the wave (generally different from ω)
 χ = angle of encounter
 μ = exponential attenuation with the mean depth of the particles.

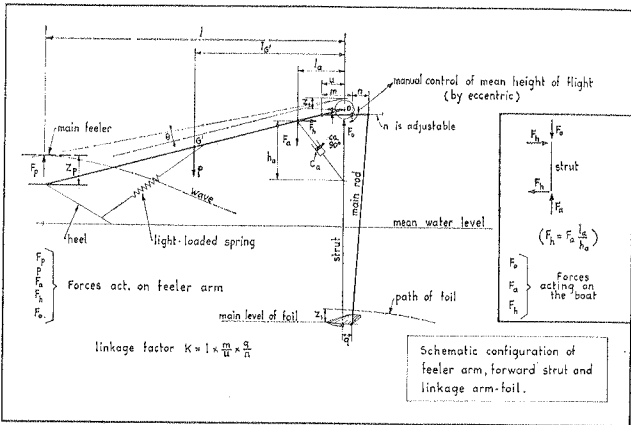


Figure 2

Due to the vertical motions of boat and water, we have thus a sinusoidal fluctuation of the effective incidence:

$$\Delta \alpha = \frac{\dot{Z}_v - \dot{Z}}{V} = \frac{1}{V} \left(\mu \frac{\sigma H}{2} \cos \omega t - \dot{Z} \right)$$

The variation of horizontal speed does not introduce any change on the amplitude of this incidence fluctuation. It results only in a slight distortion of the basic harmonic fluctuation.

2.2.3. Effect of pitch

This effect is quite simply introduced by the pitch angle, thus:

$$\Delta \alpha = \psi$$

2.3. Lift fluctuation independent from the angle of incidence

2.3.1. Variation of horizontal speed

We just saw that the horizontal component of a particle's speed is expressed by

$$\Delta V = -\mu \frac{\sigma H}{2} \cos \chi \sin \omega t$$

Since the derivative of the lift as function of the speed is given by

$$C_L \rho V S$$

we may write, in first approximation:

Lift fluctuation due to $\Delta V =$
 $-C_L \rho V S \mu \frac{\sigma H}{2} \cos \chi \sin \omega t$

2.3.2. Effect of direct coupling due to the shock-absorber

The dashpot sketched on figs. 1 and 2 is of primary importance for governing the amplitudes of the arm motions and thus the rate $\frac{da}{dt}$. It is clear that, if they are not restrained in some such way, the amplitudes may become completely "wild", with important foil cavitation effects.

Examination of fig. 2 shows that a relative vertical displacement between feeler and forward strut corresponds to an angle given approximately by

$$\theta = \frac{Z_p - Z_l}{l}$$

for small oscillations.

Further, the vertical reaction to the displacement of the dashpot is:

$$F_a = c_a l_a \dot{\theta}$$

Wherein: c_a = characteristic of the shock absorber, supposed to work proportionately to the speed of displacement in first approximation.

The equations of equilibrium of the arm are then:

$$F_p - p - c_a l_a \dot{\theta} + F_o = \frac{p}{g} l_G' \ddot{\theta}$$

$$F_p \cdot l - p l_G' - c_a l_a^2 \dot{\theta} = I_p \ddot{\theta}$$

wherein: p = weight of complete arm

I_p = moment of inertia of the arm, about the axis of rotation (O).

The resulting vertical force acting upward on the boat is given by:

$$c_a l_a \dot{\theta} - F_o = F_p - p - \frac{p}{g} l_G' \ddot{\theta}$$

(1) This does not mean that it will effectively be so, since the orbital motion of particles introduces a continuous lift fluctuation. Further, for 2 ft waves, the arms will be forced to move by the heels, even without contact between surface and feelers.

(2) and consequently, for all longer waves.

Replacing F_p by its expression in the moment equation we get:

$$c_a l_a \dot{\theta} - F_o = p \left(\frac{l_G}{l} - 1 \right) + c_a \frac{l_a^2}{l} \dot{\theta} + \left(\frac{l_p}{l} - \frac{p}{g} l_G' \right) \ddot{\theta}$$

Up to now, and concerning the boat as a whole, we have spoken of lift variations, neglecting the static equilibrium between weight and mean buoyancy. Here we have introduced the weight p , and this is why it appears explicitly in the form

$p \left(\frac{l_G'}{l} - 1 \right)$, which is simply that part of the arm weight taken by the boat. This weight fraction being now considered as a part of the boat weight, may disappear from our notations.

We still have to appraise the value of the terms in $\dot{\theta}$ and $\ddot{\theta}$. Let us first study the second one. Supposing that the arm weight is uniform along its length, we obtain for the coefficient of $\ddot{\theta}$:

$$\frac{p}{g} \left(-\frac{1}{6} \right)$$

We take again the example of the K 2 (1) to get an idea of the order of magnitude of that term, compared with the main force due to lift. Let us assume that the double amplitude of the feelers' vertical oscillation will be 40 cm. With a linkage factor $K = 3$, the amplitudes of the incidence variation will be:

$$\frac{0,20}{3} = 0,0666 \text{ rad. } (2)$$

With $C'_L = 3,50$ (a normal average value), $V = 15,45$ m/sec. (30 knots) and a foil surface of $0,15 \text{ m}^2$, we find that, in salt water ($\rho = 104,5$), the magnitude of oscillatory lift will be 435 kg.

Now the max. angular acceleration of the arm, for $\omega = 4$ and $l = 2,60$ m. will be

$$\theta_{\max} = \frac{0,20 \times (4)^2}{2,60} = 1,23 \text{ rad/sec.}^2$$

Since each complete feeler-unit weighs only some 30 kg., the $\ddot{\theta}$ term gives abt 1,63 kg., i.e., 0,37 per cent of the main effect. Now we shall find something comparable for the $\dot{\theta}$ term, i.e., the shock-absorber effect.

In the same hypotheses, $(\dot{\theta})_{\max} = \frac{0,20 \times 4}{2,60} = 0,308 \text{ rad/sec.}$

with $c_a = 1.000 \text{ kg/m/sec.}$ and $l_a = 0,30 \text{ m.}$, we obtain:

$$1.000 \times \frac{(0,30)^2}{2,60} \times 0,308 = 10,7 \text{ kg.}$$

This is hardly 2,5 per cent of the main effect.

Let us emphasize the necessary restrictions on that conclusion: it does not mean at all that the presence of the shock-absorbers will not, as claimed by Mr. Hook, ensure an effective anti-crash action. In extreme cases of a very steep wave met just after ventilation of the foils, the respective importance of the orders of magnitudes may be, for a short time, completely reverted. (See appendix for more details about the crash prevention.)

3. The coupled equations of heave and pitch of a "Hydrofin".

Having expressed the different forces acting on the boat, and eliminated the secondary effects, we shall be soon ready to write the complete linear differential equations, but firstly we have to give some definitions in order to pass from the preceding considerations, valid for one foil, to the general case of the boat, for which we need to introduce the phase lag between the different points of the system water-foils-hull.

Referring once more to fig. 1, we assume that the sinusoidal wave travels at a speed of $1,25 \sqrt{\lambda} (1)$ in the positive direction of the x-axis.

On the figure, the boat is represented flying in the same direction, but we must imagine that the given sketch may become the projection of the actual boat on the plane of the figure, i.e., the plane perpendicular to the generating line of the wave pattern. In that case, any actual dimension must be multiplied by $\cos \chi$ and χ is called the angle of encounter ($\chi = 0^\circ$ on the figure).

The speed of encounter boat — waves, or preferably, the apparent

(1) If the motions of the boat are totally restrained: this is again a simplified reasoning, only of comparative value.

(2) See Table 2.

(3) According to the theory of trochoidal waves.

speed of the waves for the boat is $(1,25 \sqrt{\lambda} - V \cos \chi)$, positive with the x-axis, so that the circular frequency of encounter is expressed by

$$\omega = \frac{2\pi [1,25 \sqrt{\lambda} - V \cos \chi]}{\lambda}$$

At the centre of gravity and at a given moment there is a rise of the surface equal to:

$$Z_v = \frac{H}{2} \sin \omega t$$

It should be remembered that this expression may be represented by the projection, on a vertical axis, of a vector of modulus $\frac{H}{2}$

turning at an angular speed ω , and being horizontal for $t = 0$,

$$t = \frac{\pi}{\omega}, t = \frac{2\pi}{\omega}, \text{ and so on.}$$

Now, for a point of the boat located at a distance ξ from the centre of gravity (positive forward of that point), the rise of the surface will lag behind by an angle equal to

$$\frac{\xi \cos \chi}{\lambda} 2\pi$$

so that:

$$(Z_v)_\xi = \frac{H}{2} \sin \left(\omega t - \frac{\xi \cos \chi}{\lambda} 2\pi \right) \\ = \frac{H}{2} \sin \left[\omega \left(t - \frac{\xi \cos \chi}{1,25 \sqrt{\lambda} - V \cos \chi} \right) \right]$$

This case will correspond to a vector of the same modulus as the first, but making an angle with it equal to: $\frac{\xi \cos \chi}{\lambda} 2\pi$

It is interesting to verify this relation for different cases. Let us first assume that the boat flies with the waves, but slower than

them. Then ω is positive, as is $\frac{\xi \cos \chi}{\lambda} 2\pi$, for any point forward

of the centre of gravity, and it will indeed take a certain time before a given rise of the surface under G reaches a point forward of it. If we now suppose that the boat is faster than the

waves, we find that ω is negative, whereas $\frac{\xi \cos \chi}{\lambda} 2\pi$ remains

positive, and the lag behind becomes an advance, which was to be expected, because the bow reaches any given point of the waves before the centre of gravity.

Finally, if the boat runs against the waves, then ω is positive again since $\cos \chi = -1$ but for the same reason $\frac{\xi \cos \chi}{\lambda} 2\pi$

becomes negative, and we find as expected, that the bow is again in advance of phase in respect to G.

For the three most important stations on the boat length, we get:

1. For the feelers

$$(Z_v)_p = \frac{H}{2} \sin \left[\omega t - \frac{(l + r_1) \cos \chi}{\lambda} 2\pi \right]$$

2. For the forward foils:

$$(Z_v)_1 = \frac{H}{2} \sin \left[\omega t - \frac{r_1 \cos \chi}{\lambda} 2\pi \right]$$

3. for the rear foils:

$$(Z_v)_2 = \frac{H}{2} \sin \left[\omega t + \frac{r_2 \cos \chi}{\lambda} 2\pi \right]$$

wherein the dimensions r_1 , r_2 and l are always positive.

As regards the boat motions, they will be split up into a vertical translation of the centre of gravity (= heave) and a rotation around a transverse horizontal axis through that point (= pitch). At any instant, the vertical displacement of a given point of the boat (positive upward) will be given by:

$$Z_{\xi} = Z + \xi \psi$$

Equation of forces

Here we have to make an important assumption about the motion of the feeler-arms. The amplitude of that motion is, a priori, unknown, but may be chosen arbitrarily, since it is one of the aims of this study to determine the range of amplitudes (and of linkage factors), which have to be obtained for optimum characteristics of flight.

The method of finding the required amplitude for each case of wave pattern, speed, etc., is then an "a posteriori" calculation

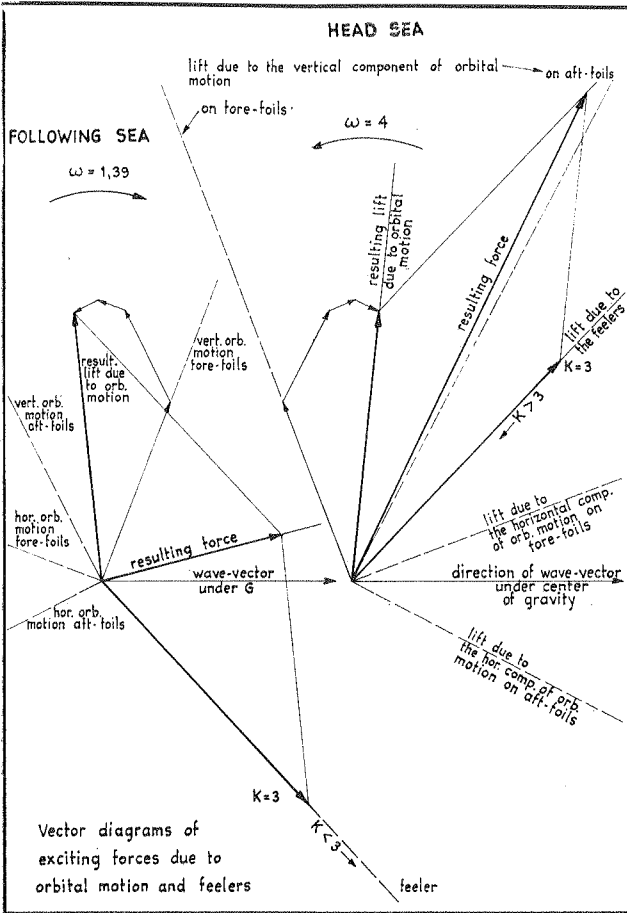


Figure 3

of the arms' characteristics (lift on feelers, range of damping, characteristics of the dashpots, etc.). The phase lag of the feeler motion in respect to the wave is another unknown, but it seems acceptable to assume that it will generally not be very large, the damping and inertia forces being small compared to the lift forces on the feelers.

Finally, the impulses on the latter are not sinusoidal, but it seems however acceptable to approach the question by assuming that the vertical heave of the feeler will be given, in first approximation, by:

$$(Z_p)_{\max} \sin \left[\omega t - \frac{(l + r_1) \cos \chi}{\lambda} 2\pi \right]$$

this being the first and most significant term of a Fourier series.

Thus we may write:

forward foils

$$\left\{ \begin{aligned} & (C'_L)_1 \frac{1}{2} \rho V^2 S_1 \left[\frac{1}{K} \left[(Z_p)_{\max} \sin \left(\omega t - \frac{(l + r_1) \cos \chi}{\lambda} 2\pi \right) - (Z + r_1 \psi) \right] \right. \\ & \left. + \psi + \frac{1}{V} \left[\mu \frac{\sigma H}{2} \cos \left(\omega t - \frac{r_1 \cos \chi}{\lambda} 2\pi \right) - (\dot{Z} + r_1 \dot{\psi}) \right] \right] - C_{L1} \rho V S_1 \mu \frac{\sigma H}{2} \cos \chi \sin \left(\omega t - \frac{r_1 \cos \chi}{\lambda} 2\pi \right) \end{aligned} \right.$$

rear foils

$$\left\{ \begin{aligned} & + (C'_L)_2 \frac{1}{2} \rho V^2 S_2 \left\{ \psi + \frac{1}{V} \left[\mu \frac{\sigma H}{2} \cos \left(\omega t + \frac{r_2 \cos \chi}{\lambda} 2\pi \right) - (\dot{Z} - r_2 \dot{\psi}) \right] \right\} \\ & - C_{L2} \rho V S_2 \mu \frac{\sigma H}{2} \cos \chi \sin \left(\omega t + \frac{r_2 \cos \chi}{\lambda} 2\pi \right) \end{aligned} \right.$$

inertia $-\frac{P}{g} \ddot{Z} = 0$

After division of all the terms by $\frac{1}{2} \rho V^2 S C'_L$ (assuming that $(C'_L)_1 = (C'_L)_2 = C'_L$), we write an equation of the well-known form:

$$AZ + B\ddot{Z} + C\ddot{\psi} + D\dot{\psi} + E\dot{\psi} + F\dot{\psi} = G \sin(\omega t + \beta p) + H_1 \cos(\omega t + \beta_1) + H_2 \cos(\omega t + \beta_2) + J_1 \sin(\omega t + \beta_1) + J_2 \sin(\omega t + \beta_2)$$

wherein A, B, C, etc., are given in table 2. whereas:

$$\beta_1 = \frac{r_1 \cos \chi}{\lambda} 2\pi$$

$$\beta_2 = + \frac{r_2 \cos \chi}{\lambda} 2\pi$$

$$\beta_p = - \frac{(r_1 + l) \cos \chi}{\lambda} 2\pi$$

It is interesting to give a graphical representation of the second member, for two typical cases, head and following seas in the hypotheses already mentioned applied to a small boat as the K 2 ($\lambda = 36$ m., $H = 1$ m., $V = 15,45$ m/sec., $K = 3$ and $Z_p = 0,20$ m.).

For that drawing of qualitative interest, we assumed no attenuation of waves ($\mu = 1$). The diagrams of fig. 3 clearly show the "anticipation" of the feelers, the vector due to the feeler being always in advance on the vector wave under the centre of gravity.

This advance is particularly welcome in case of following sea, since the resulting lift vector due to the orbital motion lags about 90° behind the wave vector.

The resulting effect "feeler + orbital motion" can be made practically in phase with the wave by an appropriate choice of K.

Now, if we have to decrease the linkage factor (thus increasing the response) for a following sea, the opposite is likely to be required for head seas, since then the resulting vector due to orbital motions is in advance of phase, and we do not wish the boat to experience excessive and unnecessary exciting forces. It seems to the writer that those two diagrams (fig. 3) are the best illustration of the advantages offered by the "Hydrofins" and other boats provided with effectively anticipating incidence controls.

Coefficients of the equations of motions.	
Equations of forces	Equation of moments
1 st member	1 st member
$A = \frac{1}{K} \cdot \frac{S_1}{S}$	$a = \frac{1}{K} \cdot \frac{S_1}{S} \cdot \frac{r_1}{r} = A \frac{r_1}{r}$
$B = \frac{1}{V}$	$b = \frac{1}{V} \cdot \frac{S_1 r_1 - S_2 r_2}{S r}$
$B_1 = \frac{1}{V} \cdot \frac{S_1}{S}$	$c = 0$
$B_2 = \frac{1}{V} \cdot \frac{S_2}{S}$	$d = \left(\frac{1}{K} r_1 - 1 \right) \frac{S_1}{S} \cdot \frac{r_1}{r} + \frac{S_2 r_2}{S r}$
$C = \frac{C_L}{C'_L} \cdot \frac{1}{g}$	$e = \frac{1}{V} \left(\frac{S_1 r_1^2 + S_2 r_2^2}{S r} \right)$
$D = \left(\frac{1}{K} r_1 - 1 \right) \frac{S_1}{S} - \frac{S_2}{S}$	$f = \frac{C_L}{C'_L} \cdot \frac{1}{g} \cdot \frac{i^2}{r} = C \cdot \frac{i^2}{r}$
$D_1 = \left(\frac{1}{K} r_1 - 1 \right) \frac{S_1}{S}$	
$D_2 = - \frac{S_2}{S}$	
$E = \frac{1}{V} \cdot \frac{S_1 r_1 - S_2 r_2}{S}$	
$E_1 = \frac{1}{V} \cdot \frac{S_1 r_1}{S} = B_1 r_1$	
$E_2 = - \frac{1}{V} \cdot \frac{S_2 r_2}{S} = - B_2 r_2$	
$F = 0$	
2 ^d member	2 ^d member
$G = \frac{1}{K} \cdot \frac{S_1}{S} (Z_p)_{\max} = A (Z_p)_{\max}$	$g = G \frac{r_1}{r}$ feeler
$H_1 = \frac{1}{V} \cdot \frac{\sigma H}{2} \cdot \frac{S_1}{S} \mu$	$h_1 = H_1 \frac{r_1}{r}$
$H_2 = \frac{1}{V} \cdot \frac{\sigma H}{2} \cdot \frac{S_2}{S} \mu$	$h_2 = -H_2 \frac{r_2}{r}$
$J_1 = - \frac{1}{V} \cdot \cos \chi \cdot \frac{\sigma H}{2} \cdot \frac{C_{L1}}{C'_L} \cdot \frac{S_1}{S} \mu$	$j_1 = J_1 \frac{r_1}{r}$
$J_2 = - \frac{1}{V} \cdot \cos \chi \cdot \frac{\sigma H}{2} \cdot \frac{C_{L2}}{C'_L} \cdot \frac{S_2}{S} \mu$	$j_2 = -J_2 \frac{r_2}{r}$
	vertical component of orbital motion
	horizontal component of orbital motion

Table 2

Equations of motions for algebraic resolution.

- (1) $(A - \omega^2 C) Z_c - (\omega B) Z_s + (D - \omega^2 F) \psi_c - (\omega E) \psi_s =$
 $G \cos \beta_p - H_1 \sin \beta_1 - H_2 \sin \beta_2 + J_1 \cos \beta_1 + J_2 \cos \beta_2$
- (2) $(\omega B) Z_c + (A - \omega^2 C) Z_s + (\omega E) \psi_c + (D - \omega^2 F) \psi_s =$
 $G \sin \beta_p + H_1 \cos \beta_1 + H_2 \cos \beta_2 + J_1 \sin \beta_1 + J_2 \sin \beta_2$
- (3) $(a - \omega^2 c) Z_c - (\omega b) Z_s + (d - \omega^2 f) \psi_c - (\omega e) \psi_s =$
 $g \cos \beta_p - h_1 \sin \beta_1 - h_2 \sin \beta_2 + j_1 \cos \beta_1 + j_2 \cos \beta_2$
- (4) $(\omega b) Z_c + (a - \omega^2 c) Z_s + (\omega e) \psi_c + (d - \omega^2 f) \psi_s =$
 $g \sin \beta_p + h_1 \cos \beta_1 + h_2 \cos \beta_2 + j_1 \sin \beta_1 + j_2 \sin \beta_2$
- (5) $Z_G = \sqrt{Z_s^2 + Z_c^2}$
- (6) $\psi_G = \sqrt{\psi_s^2 + \psi_c^2}$

to be calculated:	Z_s	ψ_s
	Z_c	ψ_c
	Z_G	ψ_G

Table 3

Equation of moments

The equation of moments is similar to the equation of forces. The term concerning the forward foils in the latter is multiplied by r_1 , whereas the term of the rear foil is multiplied by

$(-r_2)$. Of course the term of inertia becomes $-\frac{P}{g} i^2 \ddot{\psi}$,

where i is the longitudinal radius of inertia.

After dividing by $\frac{1}{2} \rho V^2 S r C'_L$, we find a second equation of the form:

$$aZ + b\ddot{Z} + c\ddot{\psi} + d\dot{\psi} + e\dot{Z} + f\dot{\psi} = g \sin(\omega t + \beta_p) + h_1 \cos(\omega t + \beta_1) + h_2 \cos(\omega t + \beta_2) + j_1 \sin(\omega t + \beta_1) + j_2 \sin(\omega t + \beta_2)$$

wherein a, b, c, \dots , are also given in table 2. (1)

This system of two differential equations may be replaced by another system of four equations with four unknowns namely Z_c, Z_s, ψ_c and ψ_s , which are respectively the real and imaginary parts of the heave and pitch vectors, the real part having the same support and positive direction as the wave vector for a point located under the boat centre of gravity.

The amplitude of heave is therefore: $Z_G = \sqrt{Z_s^2 + Z_c^2}$ and the amplitude of pitch: $\psi_G = \sqrt{\psi_s^2 + \psi_c^2}$, whereas the tg. of the angle of phase between those motions and the wave amplitude under G is given respectively by $\frac{Z_s}{Z_c}$ and $\frac{\psi_s}{\psi_c}$ (see table 3).

4. Oscillating vertical forces acting on the wings.

When, for given parameters, we have calculated the unknowns in the foregoing paragraph, we can easily determine the amplitude of the oscillatory forces on the foils by "picking-up" separately, in the equation of forces, the terms corresponding to fore and aft foils.

The expression of F_1 and F_2 are given in table 4, as is the expression of the amplitude of the resulting force F_r , which must be equal to $\frac{P}{g} \omega^2 Z_G$, a useful control for our future numerical computations.

This appraisal of the dynamic component of the forces is, of course, of primary importance for the scantlings of the struts, since they are of the same order of magnitude as the static reactions.

5. Mean level of flight, minimum motions and minimum immersion of foils

The solution of the equations of motions allows us to find the

(1) The symbol g is used for two different purposes. As the amplitude of the first exciting moment, and also as the acceleration of gravity. The author apologizes for this coincidence which is not likely to be misleading.

range of $(Z_p)_{\max}$ and K likely to give the best responses in the majority of the cases. An optimum response means not only as small motions as possible, but also motions which are compatible, in amplitude as in phase, with the basic requirements, i.e., the absence of broaching and slamming. The first requirement means that the difference between instantaneous vertical displacements of foil and water surface, must always be inferior to the mean level of immersion h_m (see fig. 4). It is however not sufficient that the foil just does not reach the surface. To avoid cavitation and ventilation, we have to comply with a certain absolute minimum of immersion $(h_o)_{\min}$.

This condition may be expressed by stating that the vectorial difference between wave and corresponding wing $(Z_v)_{1,2} - Z_{1,2}$ must be inferior or equal to $h_m - (h_o)_{\min}$.

On the other hand, the avoidance of slamming requires that the same vectorial difference between wave and foil be inferior or equal to $h_s - h_m$ (see fig. 4).

The relations used for this calculation are collected in table 5.

6. General lines of the computing work.

We are now in a position to outline the general calculation procedure.

Starting from the basic data for a given boat, such as foils areas and location, weight, etc. . . we let two of them systematically vary, defining the feeling devices, i.e. $(Z_p)_{\max}$ and K , for a series of interesting wave patterns and angles of encounter.

For instance, with the main particulars of the K 2 (table 1), we take the wave type already mentioned ($\lambda = 36$ m. and $H = 1$ m.) and, assuming that $(Z_p)_{\max} = 0,20$ m., we calculate — for specific cases of encounter such as $\chi = 0^\circ, \chi = 45^\circ$ and $\chi = 180^\circ$ — the values of the amplitudes $(Z_1)_{\max}$ and $(Z_2)_{\max}$ as functions of K .

These functions will be put into diagrams, as well as the functions

$$[(Z_v)_1 - Z_1]_{\max} \text{ and } [(Z_v)_2 - Z_2]_{\max}$$

By adding up the minimum immersion $(h_o)_{\min}$ to the greater of the last mentioned functions, we get another curve which represents $(h_m)_{\min}$, i.e., the min. value of the mean immersion. A last curve will represent $h_s - (h_m)_{\min}$.

All values of K for which the last curve lies under one of the $[(Z_v)_{1,2} - Z_{1,2}]_{\max}$ will be excluded as giving contact between wave and hull⁽²⁾. The value of K will therefore be chosen so as to avoid this, but for as small $(Z_1)_{\max}$ and $(Z_2)_{\max}$ as possible. It is clear that such a systematic method will enable us to determine the range of linkage factors which must be available. On the other hand, the mean levels of immersion will determine the characteristics of the manual foils control which causes the craft to be flown lower or higher.

By doing the outlined work for different $(Z_p)_{\max}$ it will be possible to investigate the influence of the feeler motion, which may be controlled by the feelers incidence and by the variation of the damping characteristics of the dashpots.

Finally it must be noticed that the attenuation factor μ has to be calculated approximately, assuming a mean immersion which

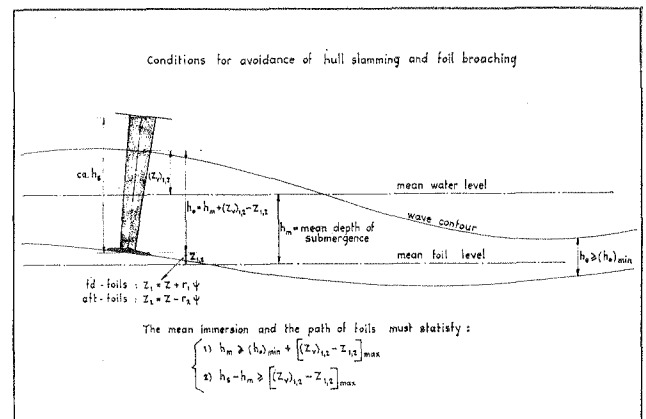


Figure 4

(2) More simply, the range of allowable K may be obtained by using the inequality: $[(Z_v)_{1,2} - Z_{1,2}]_{\max} \leq \frac{1}{2} [h_s - (h_o)_{\min}]$ (see table 5)

is not already defined. However, a percentage of error on that factor is not too significant in respect of the other approximations. For the K 2 we should assume $\mu = 0,90$ for all cases. This corresponds to a mean immersion of 60 cm.

7. Some examples of the numerical results obtained for the K2.

Diagrams 5, 6 and 7a give the results of some calculations carried out with a digital electronic computer. They apply to the case of a hydrofin type K 2 (according to the data of table 1) flying in sinusoidal waves defined by:

$$\lambda = 36 \text{ m. and } H = 1,00 \text{ m.}$$

Other main data are: $C'_L = 3,94$, $Z_p = 0,20$ m. and $\mu = 0,90$. The computing work was also carried out for $C'_L = 3,50$ and $\mu = 1,00$. This has clearly demonstrated that these small variations are of negligible influence. Generally speaking, we may say that passing from $C'_L = 3,94$ to $C'_L = 3,50$ decreases slightly the boat motions in the same conditions, whereas replacing $\mu = 0,90$ by $\mu = 1,00$ means a small increase of the motions. In no case is there a change in the orders of magnitude, which would modify the general conclusions we may draw from the graphs⁽¹⁾:

1. By adopting a value of abt 6 for K in following sea ($\chi = 0^\circ$) we are ensured of a comfortable ride, without broaching, since the minimum immersion will be 40 cm., and without slamming, as:

$$h_s - (h_m)_{\min} = \text{abt } 50 \text{ cm.} > [(Z_v) - Z]_{\max} = \text{abt } 20 \text{ cm.}$$

There is thus a reserve of abt 30 cm. between keel and wave surface. Further, the accelerations are quite acceptable:

$$(\ddot{Z}_1)_{\max} = \text{abt } 0,50 \times (-1,387)^2 = 0,96 \text{ m/sec}^2 = \text{abt } 0,1 \text{ g.}$$

2. The linkage factor $K = 6$ may remain unchanged in a quartering sea ($\chi = 45^\circ$). However, at the aft foil, the distance between bottom and water surface becomes somewhat marginal. Better results will be obtained by reducing the response of the foils: $K = 9$ seems to be the optimum setting.

Here again, there is no problem of comfort: the amplitude of motions is of the same order as in the previous case, whereas the frequency of encounter is much smaller.

3. The third case (fig. 7a, head sea, $\chi = 180^\circ$), is not so favourable as the previous ones: the range of acceptable K is very small, from $K = 1$ to $K = 2,8$. Moreover, the vicinity of the resonance peak means that a small error in the adjustment of K is likely to make the flight much less comfortable than expected ! Already for $K=1$, the max. acceleration of the aft. foil will be abt. 0,7 g, and becomes 1,3 g. for $K = 2,8$! Even if the foils are calculated for supporting the forces associated with such accelerations, it will perhaps be nice sport, but not the best way to attract ordinary customers.

There is another danger in the proximity of the resonance peak: we can see, by comparing the three diagrams, that the own frequency of the boat increases with decreasing K. Therefore, waves which are somewhat shorter than 36 m. will rapidly shift the resonance peak towards the chosen K.

Finally, a systematic variation of $(Z_p)_{\max}$ (fig. 7b and 7c) show that a strong coupling of feeler and foil in head sea makes the

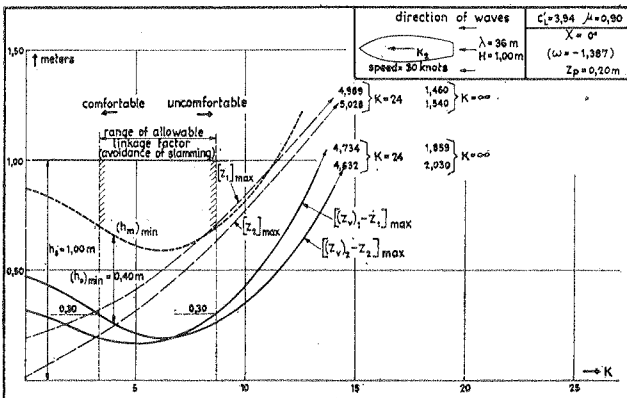


Figure 5

⁽¹⁾ This slight influence of variations of C'_L and μ is most welcome, since it is rather difficult to assess exact values at the project stage.

Equations of forces.

Vertical forces on forward foils :

$$\frac{(F_1)_c}{\frac{1}{2} \rho V^2 S C'_L} = [G \cos \beta_p - H_1 \sin \beta_1 + J_1 \cos \beta_1] - [AZ_c - \omega B_1 Z_s + D_1 \psi_c - \omega E_1 \psi_s]$$

$$\frac{(F_1)_s}{\frac{1}{2} \rho V^2 S C'_L} = [G \sin \beta_p + H_1 \cos \beta_1 + J_1 \sin \beta_1] - [AZ_s + \omega B_1 Z_c + D_1 \psi_s + \omega E_1 \psi_c]$$

$$F_1 = \sqrt{(F_1)_s^2 + (F_1)_c^2}$$

Vertical forces on aft foils :

$$\frac{(F_2)_s}{\frac{1}{2} \rho V^2 S C'_L} = [-H_2 \sin \beta_2 + J_2 \cos \beta_2] - [\omega B_2 Z_s + D_2 \psi_c - \omega E_2 \psi_s]$$

$$\frac{(F_2)_c}{\frac{1}{2} \rho V^2 S C'_L} = [H_2 \cos \beta_2 + J_2 \sin \beta_2] - [\omega B_2 Z_c + D_2 \psi_s + \omega E_2 \psi_c]$$

$$F_2 = \sqrt{(F_2)_s^2 + (F_2)_c^2}$$

Control : $F_r = \sqrt{F_s^2 + F_c^2} = \frac{P}{g} \omega^2 Z_p$

wherein $F_s = (F_1)_s + (F_2)_s$ and $F_c = (F_1)_c + (F_2)_c$

to be calculated :		
$(F_1)_s$	$(F_2)_s$	F_s
$(F_1)_c$	$(F_2)_c$	F_c
F_1	F_2	F_r and $\frac{P}{g} \omega^2 Z_p$

Table 4

boat very sensitive to the possible variations in the amplitude of the feeler motions. Indeed, for $(Z_p)_{\max} = 0,05$ m, the small range of permissible K falls exactly in the resonance peak. On the contrary, a very large $(Z_p)_{\max}$ (0,50 m.) should ask for a K less than 1, thus such a strong linkage coupling that the foil angle is greater than the feeler arm angle. Again this would lead to unacceptable accelerations.

Therefore, the right solution does not seem to be in seeking a rather unstable optimum in the low K-range but in adopting directly a high K value, thus reducing greatly the linkage between feeler and foil. By doing so the accelerations will be inferior to 0,5 g. However, the situation is still not quite satisfactory, since the avoidance of broaching and slamming will lead to accept a very small $(h_o)_{\min}$, less than 0,20 m., instead of 0,40 m. in the previous cases, so that the definitive solution before flying at top speed against such high and short crested waves will be to increase the struts height up to about 1,30 m. This seems to be a rather pessimistic statement, but we must not forget that the situation will be proportionately much easier for larger boats flying at about the same speed than the K 2, since the frequency of encounter of these boats with the waves of "boundary" height, will be considerably smaller than the value we have here, viz. $\omega = 4$.

Conclusions

The purpose of this paper was to give a summary of what is believed to be a simple and reliable method for estimating the influence of the different variables on the motions of a hydrofin in regular waves.

By a systematic variation of the linkage factor in different conditions of waves, speed, and angles of encounter, it is easy to determine the own frequency of the boat as a function of K.

It has been shown that there could be no sign of instability in a following and quartering sea if the linkage factor was properly adjusted, i.e., if the response of the controlled foils to the feelers motions was large enough to make the own frequency much higher than the frequency of encounter.

On the contrary, the response of the foils must be lessened in a head sea, the dynamic stability being sufficiently ensured by the orbital motion of the water. Of course, the value of K may not be exaggerated, since the feelers must also provide for the static stability, i.e., the mean level of flight. Moreover, it has been

Mean depth of submergence and minimum motions compatible with avoidance of slamming and broaching.

$$\left\{ \begin{array}{l} h_m \geq (Z_{v,1,2} - Z_{1,2} + (h_0)_{\min}) \\ h_s - h_m \geq (Z_{v,1,2} - Z_{1,2}) \end{array} \right. \quad \text{wherein} \quad \left\{ \begin{array}{l} Z_1 = Z + r_1 \psi \\ Z_2 = Z - r_2 \psi \end{array} \right.$$

those inequalities are always satisfied if :

$$\left\{ \begin{array}{l} [(Z_{v,1,2} - Z_{1,2})]_{\max} \leq h_m - (h_0)_{\min} \\ [(Z_{v,1,2} - Z_{1,2})]_{\max} \leq h_s - h_m \end{array} \right. \quad (*)$$

$$\left. \begin{array}{l} (Z_1)_{\max} = \sqrt{(Z_s + r_1 \psi_s)^2 + (Z_c + r_1 \psi_c)^2} \\ (Z_2)_{\max} = \sqrt{(Z_s - r_2 \psi_s)^2 + (Z_c - r_2 \psi_c)^2} \end{array} \right\} \text{ must be as small as possible}$$

$$[(Z_{v,1} - Z_1)_{\max}] = \sqrt{\left[\frac{H}{2} \sin \beta_1 - (Z_s + r_1 \psi_s)\right]^2 + \left[\frac{H}{2} \cos \beta_1 - (Z_c + r_1 \psi_c)\right]^2}$$

$$[(Z_{v,2} - Z_2)_{\max}] = \sqrt{\left[\frac{H}{2} \sin \beta_2 - (Z_s - r_2 \psi_s)\right]^2 + \left[\frac{H}{2} \cos \beta_2 - (Z_c - r_2 \psi_c)\right]^2}$$

to be calculated $(Z_1)_{\max}$ $(Z_2)_{\max}$

$[(Z_{v,1} - Z_1)_{\max}]$ $[(Z_{v,2} - Z_2)_{\max}]$

(*) These two inequalities imply that : $[(Z_{v,1,2} - Z_{1,2})]_{\max} \leq \frac{1}{2} [h_s - (h_0)_{\min}]$
(N.B.: this condition is necessary, but not sufficient.)

Table 5

demonstrated that very large variations in the feelers motions have, for the advised K-values, only a small influence on the seaworthiness of the boat: we must try to limit those motions as far as possible, but it is clear that it does not matter very much whether we succeed in getting $(Z_p)_{\max} = 0,05$ m. or $(Z_p)_{\max} = 0,20$ m. in the given example.

Another most useful conclusion concerns the influence of C'_L and μ , the estimation of which need not be made with great accuracy.

In this paper, we did not consider the influence of foils surfaces and locations, feelers arm lengths, weight of craft, radius of inertia, and so on. It is obvious that the proposed method enables us to determine the optimum values of those different parameters, but such an extensive investigation falls outside the scope of this introductory study.

Acknowledgment

The author wishes to express his gratitude to the different persons who encouraged this private study, particularly Mr. Chr. Hook and Prof. H. Barkla.

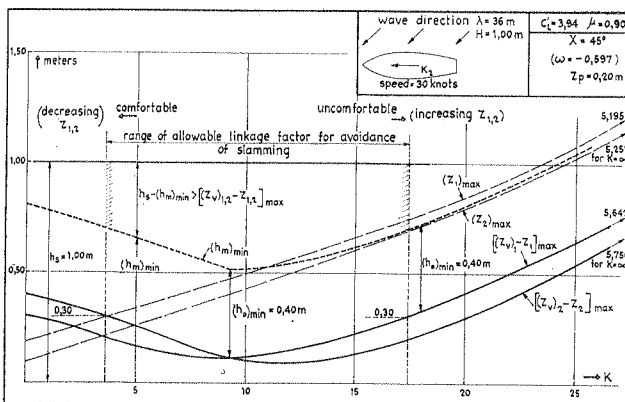


Figure 6

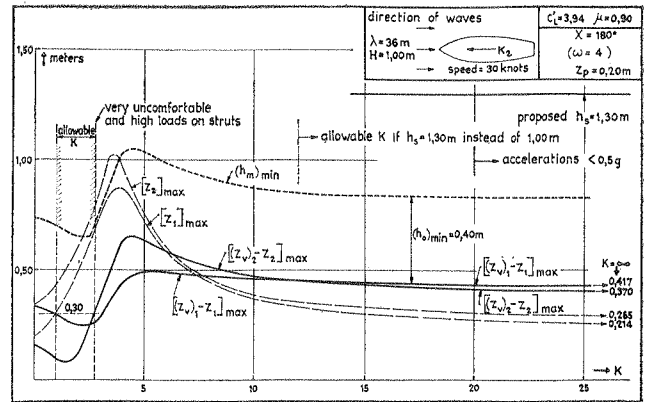


Figure 7a

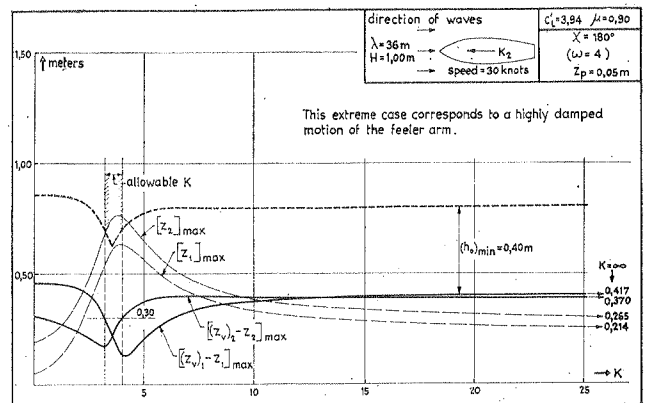


Figure 7b

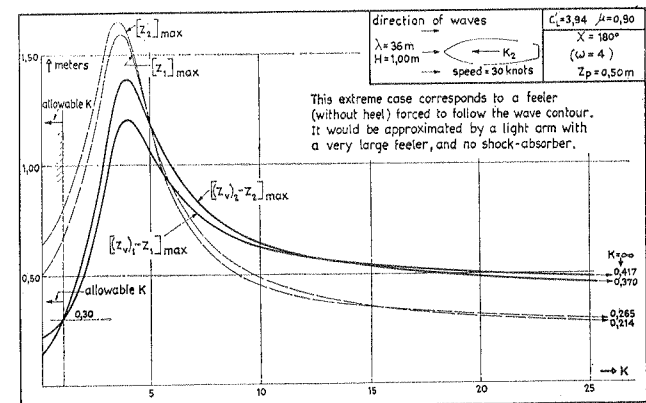


Figure 7c

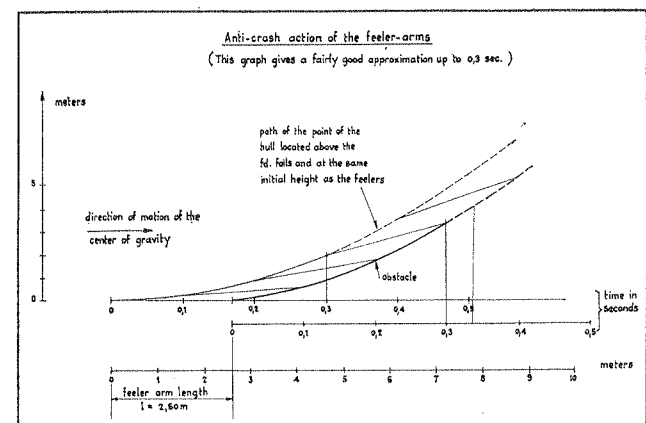


Figure 8

He is also greatly indebted to Mr. Paul Pringiers, who accepted to carry out the computing program on a IBM machine, thus reducing the calculation time by a factor of about 2'000 !

Bibliography

- [1] Chr. Hook
 "In defence of Simplicity in hydrofoil boat design".
 Hovering Craft & Hydrofoil — July, 1962.
 "Platforming ocean waves on a Hydrofoil".
 Engineering, 28th Dec., 1962.
 "Hydrofoil Personality".
 Hovering Craft & Hydrofoil — Aug./Sept., 1962.
- [2] J. Vintenon
 "Hydrofins and Hydrofoils".
 Hovering Craft & Hydrofoil — June/July, 1963
- [3] Study of Hydrofoil Seacraft.
 A report by Grumman Aircraft Engineering Corporation to
 Maritime Administration (U.S. Dept. of Commerce).

Symbols

Basic data		Units
V =	boat speed	m/sec.
S ₁ =	total surface of fd. foils, projected on a horizontal plane	m ²
S ₂ =	the same for the aft-foils	m ²
r ₁ =	horizontal distance between the centre of lift of fd. foils and the boat centre of gravity	m.
r ₂ =	the same for the aft-foils	m.
l =	horizontal distance between feelers and fd. foils	m.
K =	linkage-factor of the incidence control	m.
P =	weight of the boat	kg.
i =	longitudinal radius of inertia of the boat	m.
C' _L =	lift slope	m.
χ =	angle of encounter boat-wave (0° = following sea)	m.
λ =	wave length	m.
H =	wave height	m.
ρ =	specific mass of water = 104,5 for salt water kg. m ⁻³ -sec ²	
μ =	attenuation of the wave with depth = $\frac{1}{(2\pi h_m)\lambda}$, wherein = 2,7183	
(Z _p) _{max} =	amplitude of the vertical motions of the feelers (mean between port and starboard)	m.
Other symbols and basic formulae		
S =	S ₁ + S ₂	m ²
r =	r ₁ + r ₂	m
P ₁ =	static load of fd. foils = $\frac{Pr_2}{r}$	kg.
P ₂ =	static load of aft. foils = $\frac{Pr_1}{r}$	kg
I =	moment of inertia, about a transverse horizontal axis through G	kgm. sec ²
C _{L1} =	mean lift coefficient of fd. foils = $\frac{P_1}{\frac{1}{2} \rho V^2 S_1}$	
C _{L2} =	mean lift coefficient of aft foils = $\frac{P_2}{\frac{1}{2} \rho V^2 S_2}$	
C _L =	mean resulting lift coefficient = $\frac{P}{\frac{1}{2} \rho V^2 S}$	
σ =	circular frequency of the waves = $\frac{2\pi}{0,8 \sqrt{\lambda}}$ = 7,85 $\frac{1}{\sqrt{\lambda}}$	
ω =	circular frequency of encounter = $\frac{2\pi (1,25 \sqrt{\lambda} - V \cos \chi)}{\lambda}$	
β ₁ =	angle of phase between the wave at the fd. foils and the wave under the centre of gravity: — $\frac{r_1 \cos \chi}{\lambda} 2\pi$	

β ₂ =	the same for the aft foils = $+\frac{r_2 \cos \chi}{\lambda} 2\pi$	
β _p =	the same for the feelers = $-\frac{(l + r_1) \cos \chi}{\lambda} 2\pi$	
(Z _v) _{1,2} =	instantaneous rise of the surface at fd. or aft. foils in the plane of symmetry of the boat	m.
Z _G =	amplitude of heave = $\sqrt{Z_c^2 + Z_s^2}$	m.
ψ _G =	amplitude of pitch = $\sqrt{\psi_c^2 + \psi_s^2}$	rad.
Z _c =	projection of Z _G on the direction of the wave-vector for the point under the centre of gravity (real part of Z _G)	m.
ψ _c =	the same for ψ _G	rad.
Z _s =	component of Z _G perpendicular to Z _c (imaginary part of Z _G)	m.
ψ _s =	component of ψ _G perpendicular to ψ _c	rad.
Z _{1,2} =	instantaneous rise of fd. or aft-foils (in case of cos χ different from 1 or — 1, Z _{1,2} gives the mean rise between port and starboard)	m.
h _m =	mean submergence of the foils	m.
h _s =	length of the struts from foil to keel	m.
F ₁ =	oscillating dynamic force on fd. foils	kg.
F ₂ =	oscillating dynamic force on aft-foils	kg.
F _r =	resulting dynamic force on boat	kg.

Appendix - Some considerations about the feeler arm - shock absorber system, basic difference between action in harmonic motions and as anti-crash device.

Under par. 2.32, we have shown that, in normal conditions of flying, i.e., for waves of normal shape, the direct coupling feeler-boat through the shock-absorber gave rise to forces which are negligible compared to the magnitude of the lift variation. We then calculated a resulting oscillating vertical force on the forward struts which was given by (1)

$$c_a \frac{l_a^2}{l} \ddot{\theta} + \left(\frac{l_p}{l} - \frac{p}{g} l_G \right) \ddot{\theta}$$

Neglecting the small effect of inertia, we shall now consider the first term only.

This term may also be written $c_a \frac{l_a^2}{l^2} (\ddot{Z}_p - \ddot{Z}_1)$, and introduced in the general equation of forces. The latter offers then:

- 1. in the second member, a fifth term:

$$\frac{1}{C'_L \frac{1}{2} \rho V^2 S} c_a \left(\frac{l_a}{l} \right)^2 \omega (Z_p)_{max} \cos(\omega t + \beta_p) = Q \cos(\omega t + \beta_p)$$

- 2. in the first member, a corrective term to the coefficient B₁

$$\frac{1}{C'_L \frac{1}{2} \rho V^2 S} c_a \left(\frac{l_a}{l} \right)^2 = (B_1)_a$$

and another to D₁:

$$\frac{1}{C'_L \frac{1}{2} \rho V^2 S} c_a \left(\frac{l_a}{l} \right)^2 r_1 = (D_1)_a$$

The equation of moments has to be similarly corrected: the resulting vertical force $C_a l_a^2 \ddot{\theta}$ introduces a corresponding

moment $c_a \frac{l_a^2}{l} \ddot{\theta} r_1 = c_a \left(\frac{l_a}{l} \right)^2 (\ddot{Z}_p - \ddot{Z}_1) r_1$, whereas the horizontal component of the force on the dashpot gives another restoring moment (see fig. 2):

$$F_h \times h_a = c_a l_a \ddot{\theta} \frac{l_a}{h_a} \cdot h_a = c_a l_a^2 \ddot{\theta} = c_a \frac{l_a^2}{l} (\ddot{Z}_p - \ddot{Z}_1)$$

These two "direct-action" moments give two new terms in the equation of moments, namely:

- 1. in the second member:

$$\frac{1}{C'_L \frac{1}{2} \rho V^2 S r} \cdot c_a \left(\frac{l_a}{l} \right)^2 (r_1 + l) \omega (Z_p)_{max} \cos(\omega t + \beta_p) =$$

- 2. in the first member:

$$\frac{1}{C'_L \frac{1}{2} \rho V^2 S r} \cdot c_a \left(\frac{l_a}{l} \right)^2 (r_1 + l) \ddot{Z}$$

wherein the coefficient of \ddot{Z} is called (b₁)_a

(1) We now assume that c_a, l_p and p are compound values for both arms, as are S₁, r₁, etc.

and $\frac{1}{C'_L \frac{1}{2} \rho V^2 S r} \cdot c_a \left(\frac{l_a}{l}\right)^2 (r_1 + l) r_1 \dot{\psi}$
 wherein the coefficient of $\dot{\psi}$ is called $(d)_a$.

This complete presentation may prove useful in a later and more refined stage of the calculations. For now, we will limit ourselves to the question: what are the order of magnitudes of Q and q in respect of G and g, or better: for what frequency of encounter and damping characteristic should we take Q and q into account?

Let us assume, rather arbitrarily, that this becomes necessary when they are 10 per cent of G and g, respectively.

We write thus: $0,10 G = Q$

$$\text{With: } C'_L = 3,50 \quad l_a = 0,30 \quad Z_p = 0,20$$

$$\rho = 104,5 \quad l = 2,60 \quad c_a \text{ unknowns}$$

$$V = 15,45 \quad K = 3 \quad \omega$$

$$S = 0,46 \quad S_1 = 0,30$$

we find:

$$\frac{1}{3,50 \times 104,5 \times (15,45)^2 \times 0,46} \times \frac{(0,30)^2}{(2,60)^2} \times 0,20 \times c_a \omega =$$

$$0,10 \times \frac{0,20}{3} \times \frac{0,30}{0,46}, \text{ or:}$$

$$c_a \omega = 32,600$$

In the same hypotheses as under 2.32, i.e., c_a (compound) = 2×1000 kg/m/sec. and $\omega = 4$, we see that this is not satisfied (indeed we found that the shock-absorber action was somewhat less than 2,5 per cent of the lift effect).

Let us now assume that the frequency of encounter is twice as high, thus $\omega = 8$.

This will be the case with a wave length of ca. 16 m. (instead of 36 m. for $\omega = 4$), thus a very steep wave pattern, the ratio $\frac{H}{\lambda}$

being now $\frac{1}{16}$ instead of $\frac{1}{36}$.

Hydraulic shock absorbers give a damping force which may be proportional to the square of the relative speed. The mean specific damping is then proportional to this relative speed itself. It is thus logical that passing from $\omega = 4$ to $\omega = 8$ will double the mean damping effect, so that the product $c_a \cdot \omega$ will become, for both arms: $4000 \times 8 = 32.000$

We just saw that this result corresponds to a direct force equal to 10 per cent of the main effect. This extra lift being 90° in advance on the latter, the resulting vector will not be substantially increased, but the gain of some degrees of advance is not so negligible.

The exciting moment due to the shock absorber has a more pronounced effect than the exciting force, since the arm is $(l + r_1)$ and not simply r_1 .

In the same hypothesis (and $r = r_1 + r_2 = 4,80$ m.) we obtain: $q = \text{ca. } 0,0042$ against $g = 0,019$, thus q is abt. 22 per cent of g . It is therefore quite clear that, depending on the sea, the speed of the boat, the angle of encounter and the shock-absorbers characteristics, the effect of the latter may become significant, even without any tendency to broaching or crashing.

However, since the conditions of relatively powerful action will be met in short crested head seas, in which the effect of incidence control is to be reduced (see fig. 3 and 7), it will certainly be advisable to reduce also the shock-absorber characteristic in order to avoid excessive motions. Of course, a direct consequence of this, is that the incidence of the feelers must also be lessened.

Now, let us see the action of the shock-absorbers from the "anti-crash" point of view. We imagine that, all foils having made surface, the sole forces acting on the boat are, for a very short instant, the boat weight and the lifting forces on the feelers. We purposely take a very extreme case in assuming that the feelers may develop a vertical lift equal to the boat weight plus the force corresponding to the arm inertia. Neglecting the effect of this inertia on the resulting force on the boat itself, we obtain:

$$c_a \left(\frac{l_a}{l}\right)^2 (\dot{Z}_p - \dot{Z}_i) = P$$

which means that the path of the boat centre of gravity is a straight

line, which we assume to be horizontal. The anti-crash moment acting on the craft is:

$$c_a \left(\frac{l_a}{l}\right)^2 (\dot{Z}_p - \dot{Z}_i) (r_1 + l) = P (r_1 + l)$$

The moment equilibrium gives thus:

$$P (r_1 + l) = \frac{P}{g} i^2 \ddot{\psi}$$

Therefore the vertical speed of the fd.-foils is obtained by:

$$\dot{Z}_i = r_1 \dot{\psi} = \frac{g (r_1 + l) r_1}{i^2} t$$

Further, since:

$$\dot{Z}_p = \dot{Z}_i + \frac{P}{c_a} \left(\frac{l}{l_a}\right)^2$$

we obtain:

vertical displacement of the bow at the fd. foils:

$$Z_1 = \frac{g (r_1 + l) r_1}{i^2} \frac{t^2}{2}$$

vertical displacement of the feelers:

$$Z_p = Z_1 + \frac{P}{c_a} \left(\frac{l}{l_a}\right)^2 \cdot t$$

The most important question is again: what will be the c_a value in this particular case? In the basic considerations we assumed, for a *max.* relative speed between feeler and (restrained) fd.-foil $\omega (Z_p)_{\text{max}} = 4,0,20 = 0,80$ m/sec., a compound mean c_a equal to 2×1000 kg/m/sec. Now that the relative speed is *constant* we may assume the following values as order of magnitudes:

constant $(\dot{Z}_p - \dot{Z}_i) = 4,50$ m/sec. and a corresponding $c_a = 33.400$ kg/m/sec. which satisfies the relation:

$$\dot{Z}_p - \dot{Z}_i = \frac{P}{c_a} \left(\frac{l}{l_a}\right)^2$$

if: $P = 2000$ kg., $l = 2,60$ m., $l_a = 0,30$ (see the characteristics given in table 1).

For the same boat, we have $r_1 = 2,10$ m. and $i = \text{abt. } 1,50$ m.

$$\text{Thus: } Z_1 = \frac{9,81 \times 4,70 \times 2,10}{(1,50)^2} \times \frac{t^2}{2} = 21,5 t^2$$

and $Z_p = 21,5 t^2 + 4,50 t$.

Those two paths are put into diagrams on fig. 8, where the time is given together with the distance flown at a speed of 15,45 m/sec. (30 knots).

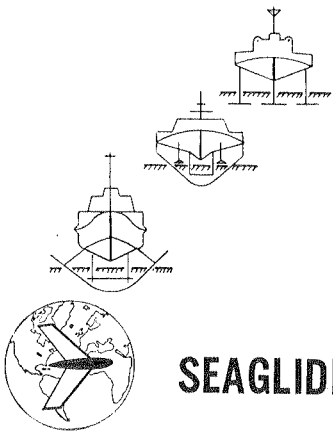
We can now see what the practical effect of the anti-crash method will be. In a fraction of a second it applies a trimming force counteracting the tendency to nose-dive and causing the boat to tend to avoid the obstacle or to encounter it with less violence. In the calculations no lift from the ventilated foil is allowed for, but this is of course an extreme case and in reality it is only necessary to substitute a new force for the loss of upper side lift due to the air. Furthermore, as the boat falls the incidence is increasing while, due to the angle of sweep the air is being shed and lift restored. The net result is then not more than a stumble and the hull generally recovers before touching the surface. How often the stumble will happen depends on how hard the boat is "pushed" in rough seas, the wave steepness, the wave encounter angle, etc., as well as the average flight path taken by the foils due to the pilot's corrective controls. Experience has proved that it is possible to so rig the incidence relative to the feeler as to render the crash impossible to produce even with the pilot trying his best. However, this line of flight will tend to be low and to present a high proportion of strut area to foil area with consequent loss of speed.

Obviously the forces thrown onto the arm in the anti-crash action call for a careful study of the scantlings of this member.

ERRATA

Figure 1. Horizontal projection of distance between centre of gravity and aft foils should read $ca.r_2$ instead of $ca.r$

Table 2. Second line, first column: Equations of forces to read "equation" of force.

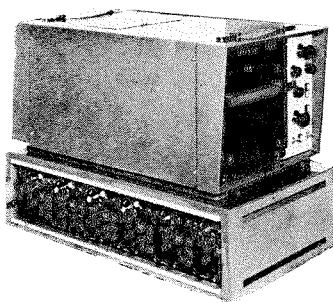


SEAGLIDER LIMITED

- Electronic & Mechanical Control Systems
- Mathematical Studies and Analyses
- Structural Design in Fibreglass
- Electronic Instrumentation
- Hydrofoil Craft Design
- Marine Electronics

Reduce design and development costs by consulting

SEAGLIDER LIMITED
 219 Sycamore Road
 Farnborough Hants



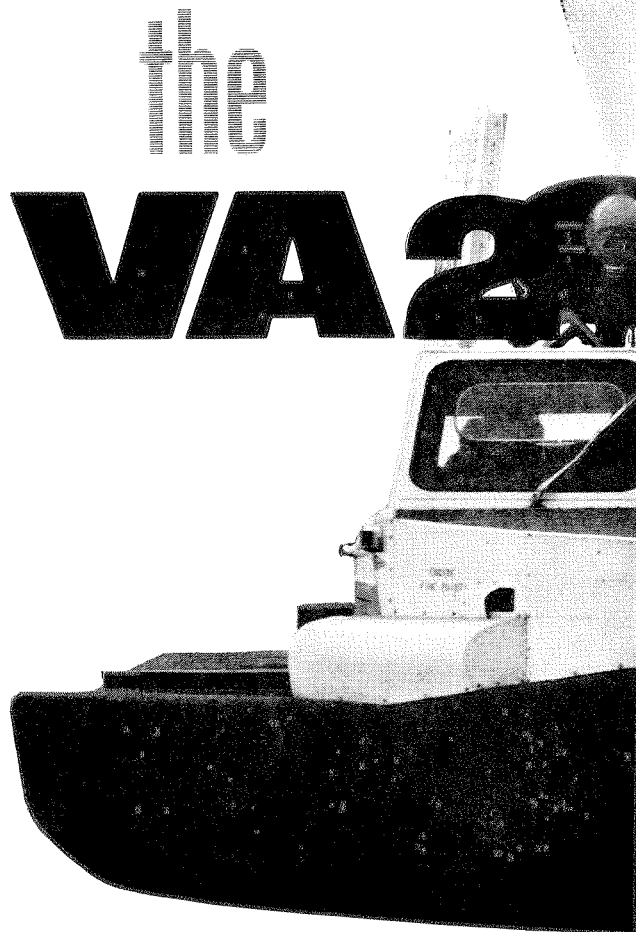
This is a Multi-Channel Ultra-Violet Recorder with Attenuator Modules package-designed to customer specification. It may be used with standard transducers, strain gauges, pressure gauges, etc.

The rapid development of your design ideas requires adequate facilities for the collection of operational data. As many phenomena have duration cycles of less than one millisecond, the job can be done efficiently only by means of electronic equipment.

Inexpensive single and multi-channel equipment, built to a wide range of customers' specifications, is our special field. For many years we have designed high and medium-speed recording apparatus which harvests and remembers information, then presents it to the designer in a manner easy to read. In consequence, we can now offer a comprehensive and tried range of recording gear which is ideal for obtaining precise results from sea-trials and proving flights. For the analysis of crash data we can supply high-g isolated magnetic wire recorders which have been tested under the severest conditions.

For the full details about these portable, fully-developed aids to marine research and their applications, consult

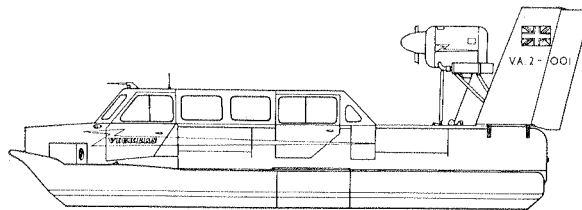
PCD - Southern Ltd
 Blackwater Station Estate
 Blackwater Camberley Surrey England



HARDY SPICER

HELPS IT TO HOVER

In the developing new field of air cushion vehicles, Hardy Spicer products are already playing their part. The lifting power for this new Vickers VA2 Hovercraft is transmitted from engines to gearboxes by two Hardy Spicer universally jointed tubular drive shafts. The VA2 has been designed to show the practical uses of Hovercraft for fast passenger and freight movements in areas where water, marsh or land are impractical for other types of transport.



HARDY SPICER

PROPELLER SHAFTS

CHESTER ROAD, ERDINGTON, BIRMINGHAM 24
 Telephone: Erdington 2191. Telex: 33414

Member of the  **Birfield Group**

54 years ago. . .

ON APRIL 2ND, 1910, an application for a patent was filed in the United States Patent Office for a "novel apparatus for transferring bodies at very high speed from one point to another". The specification of the Patent No 1,020,942 was issued on March 19th, 1912, to Emile Bachelet of Mount Vernon, Westchester, New York, and is titled "Levitating Transmitting Apparatus".

Bachelet aimed at providing a mechanically frictionless carrier floated or levitated in a magnetic field maintained around the carrier. A guideway houses the various magnets used to both float and propel the carrier, which, Bachelet states, "may be adapted for local use, such as transmitting mail and small express packages long distances at very high speed, for moving cash and parcel carriers in large department stores; and it also may be adapted in very large apparatus, for the transport of freight, or passengers".

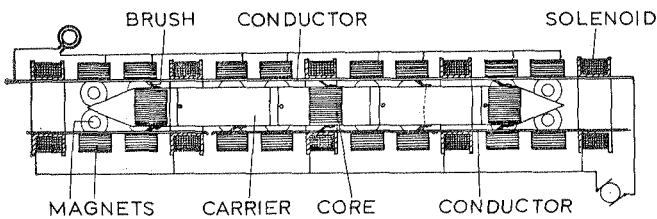


FIG. 1

Figure 1 shows the arrangement of guideway, carrier, magnets for producing a magnetic field to float the carrier and solenoids for producing translational movement. The transverse series of electro magnets is formed from opposite side magnets and a pair of base magnets arranged with alternating poles. Suitable connections are made with a source of alternating electricity as shown. The carrier is arranged to close the circuit between the conductors to energise a series of magnets and cut them out of circuit after it passes over them so that the amount of current required to operate the apparatus is kept to an economical level.

Pure aluminium or other very light conductive material is used for the carrier, the material being of sufficient thickness to resist or greatly retard the flow of magnetic lines of force so that the carrier is repelled from the magnets, the repulsion being due to the reaction of the induced eddy currents in the material of the carrier upon the field producing them. When the magnets are energised the carrier is repelled from them and remains suspended, floating in the magnetic field produced by the magnets. Solenoids which surround the path of the carrier are spaced at convenient intervals and energised in succession to draw the levitated carrier along the magnetic field at a high velocity. Some of the solenoids are arranged to brake or stop the carrier as required. For high speed passenger travel the solenoids are replaced by tractor airscrews.

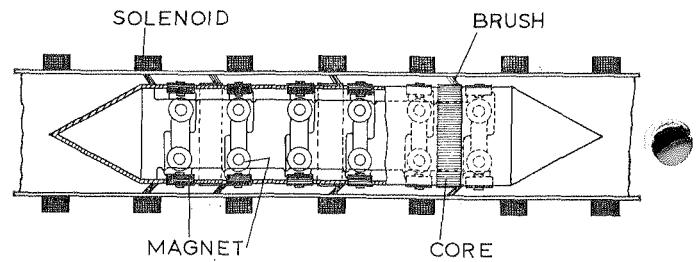


FIG. 2

Nineteen days after filing his first patent application Bachelet filed a second application which was also published on March 19th, 1912 — No 1,020,943. In the second application, shown in Figure 2, Bachelet suggested mounting the electro magnets on the carrier, the magnets being continually energised by periodic currents to levitate the carrier during movement along the guideway formed of, or lined with non-magnetic conductive material, the magnets being forcibly repelled from the guideway. The carrier contains its own source of electricity for energising the magnets or alternatively the magnets may be energised from an exterior current generator.

A third application was filed by Bachelet on February 15th, 1912, and was issued as United States Patent 1,051,056 on January 21st, 1913. This patent discloses a development of the two previous patents and is specifically related to levitating apparatus for floating safely and rapidly conveying ammunition or high explosives. The arrangement described, shown in Figure 3, operates in a similar manner to that already described with the exception that translational movement is manually imparted.

Bachelet, who patented many devices relating to electro-magnetic therapeutic apparatus, looms, pumps and an electro magnetic engine, applied his proposals for levitation for take-off and landing of aircraft. United States Patent 1,088,511, applied for in February, 1912, and patented in February, 1914, discloses a launching and landing platform for aircraft based on board ship. The aircraft and platform are levitated as described in the previous patents and the platform is moved in guideways so as to impart motion to the aircraft before take-off or on landing.

In view of the present interest in Hovercars and linear motors the patents of Bachelet may well be worth further study.

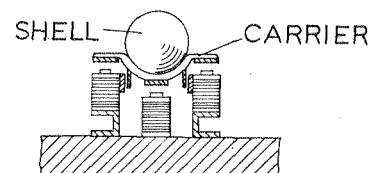
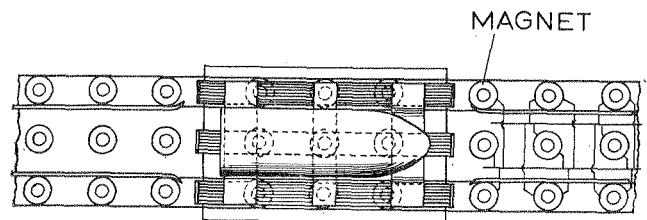
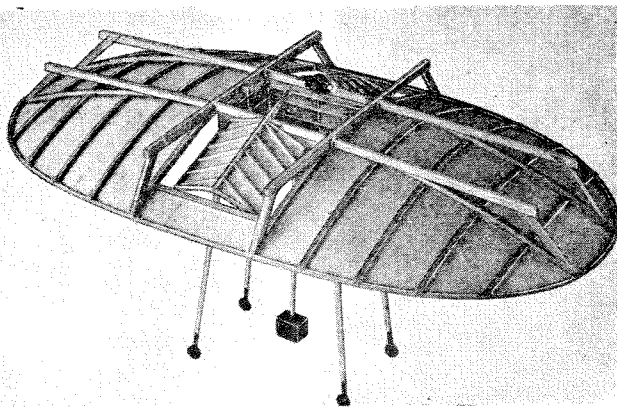


FIG. 3

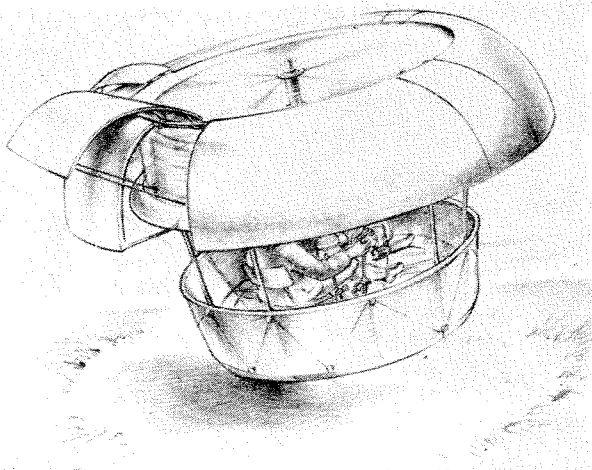


THE HISTORY OF AIR CUSHION VEHICLES

LESLIE HAYWARD

KALERGHI PUBLICATIONS

U.K. and Europe 5s. 6d. (incl. postage)
Canada and the U.S.A. \$1.25 (incl. postage)
Orders to 53-55 Beak Street, London, W.1



LEOPOLDO RODRIQUEZ
SHIPYARD
MESSINA - ITALY

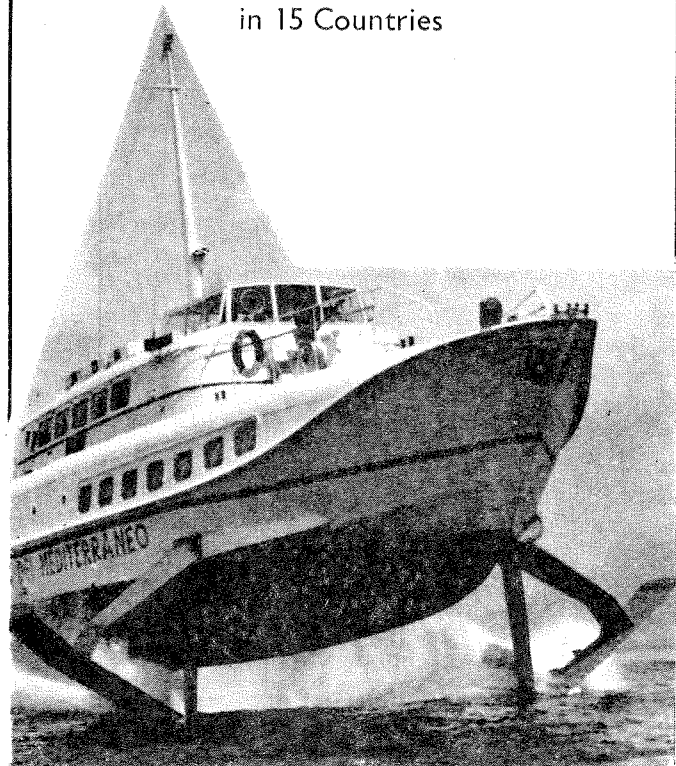


Licensed by Supramar A.G. Zug-Switzerland

The
Greatest Experience
in
Hydrofoil Boat Building

50

RODRIQUEZ
Hydrofoil Boats Across
The World's Seas
in 15 Countries



ANY KIND
of
SHIP REPAIRS